NASA TECHNICAL NOTE

NASA TN D-6687

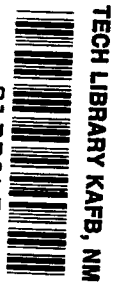

NASA TN D-6687

ANALYTICAL AND EXPERIMENTAL INVESTIGATION OF THE COAXIAL PLASMA GUN FOR USE AS A PARTICLE ACCELERATOR

by Edward L. Shriver

George C. Marshall Space Flight Center
Marshall Space Flight Center, Ala. 35812

NATIONAL AERONAUTICS AND SPACE ADMINISTRATION • WASHINGTON, D. C. • APRIL 1972

1. REPORT NO.	2. GOVERNMENT ACCESSION NO.	3. RECIPIENT'S CATALOG NO.
NASA TN D-6687		

4. TITLE AND SUBTITLE
ANALYTICAL AND EXPERIMENTAL INVESTIGATION OF THE COAXIAL PLASMA GUN FOR USE AS A PARTICLE ACCELERATOR

5. REPORT DATE
April 1972

6. PERFORMING ORGANIZATION CODE

7. AUTHOR(S)
Edward L. Shriver

8. PERFORMING ORGANIZATION REPORT #

9. PERFORMING ORGANIZATION NAME AND ADDRESS
George C. Marshall Space Flight Center
Marshall Space Flight Center, Alabama 35812

10. WORK UNIT NO.

11. CONTRACT OR GRANT NO.

12. SPONSORING AGENCY NAME AND ADDRESS
National Aeronautics and Space Administration
Washington, D. C. 20546

13. TYPE OF REPORT & PERIOD COVERED
Technical Note

14. SPONSORING AGENCY CODE

15. SUPPLEMENTARY NOTES

16. ABSTRACT

The coaxial plasma accelerator for use as a projectile accelerator is discussed. The accelerator is described physically and analytically by solution of the circuit equations, and by solving for the magnetic pressures which are formed by the $\bar{j} \times \bar{B}$ forces on the plasma.

It is shown that the plasma density must be increased if the accelerator is to be used as a projectile accelerator. Three different approaches to increasing the plasma density are discussed.

When a magnetic field containment scheme was used to increase the plasma density, glass beads of 0.66 millimeter diameter were accelerated to 7 to 8 kilometers per second velocities. Glass beads of smaller diameter were accelerated to more than twice this velocity.

17. KEY WORDS	18. DISTRIBUTION STATEMENT
Particle Acceleration Plasma Density Glass Beads	

19. SECURITY CLASSIF. (of this report)	20. SECURITY CLASSIF. (of this page)	21. NO. OF PAGES	22. PRICE
Unclassified	Unclassified	77	$3.00

For sale by the National Technical Information Service, Springfield, Virginia 22151

TABLE OF CONTENTS

TABLE OF CONTENTS (Concluded)

LIST OF ILLUSTRATIONS

LIST OF TABLES

CHAPTER I

DESCRIPTION OF THE INVESTIGATION

Introduction

Projectiles with velocities up to 10 kilometers/second are produced in the laboratory [1] and are used to study the physical processes which take place in materials impacted with very high speed projectiles. It would also be of interest to produce projectiles with velocities of 20 to 30 kilometers/second to simulate meteorite impacts. Such high velocity projectiles cannot be produced in a light gas gun like the one used in production of the 10-kilometer/second projectiles.

It has been suggested that a high velocity plasma generator might be used to accelerate projectiles to the 20-kilometer/second velocity range; this method will be discussed.

Description of Experiment

The apparatus for this experiment consisted of a capacitor bank storing 34.56 kilojoules of electrical energy at 16 kilovolts, a set of coaxial leads, an ignitron-switching bank, a coaxial plasma generator, a tubular-vacuum range, and associated instrumentation required to operate this system (Fig. 1). All of the components consisted of commercially available items

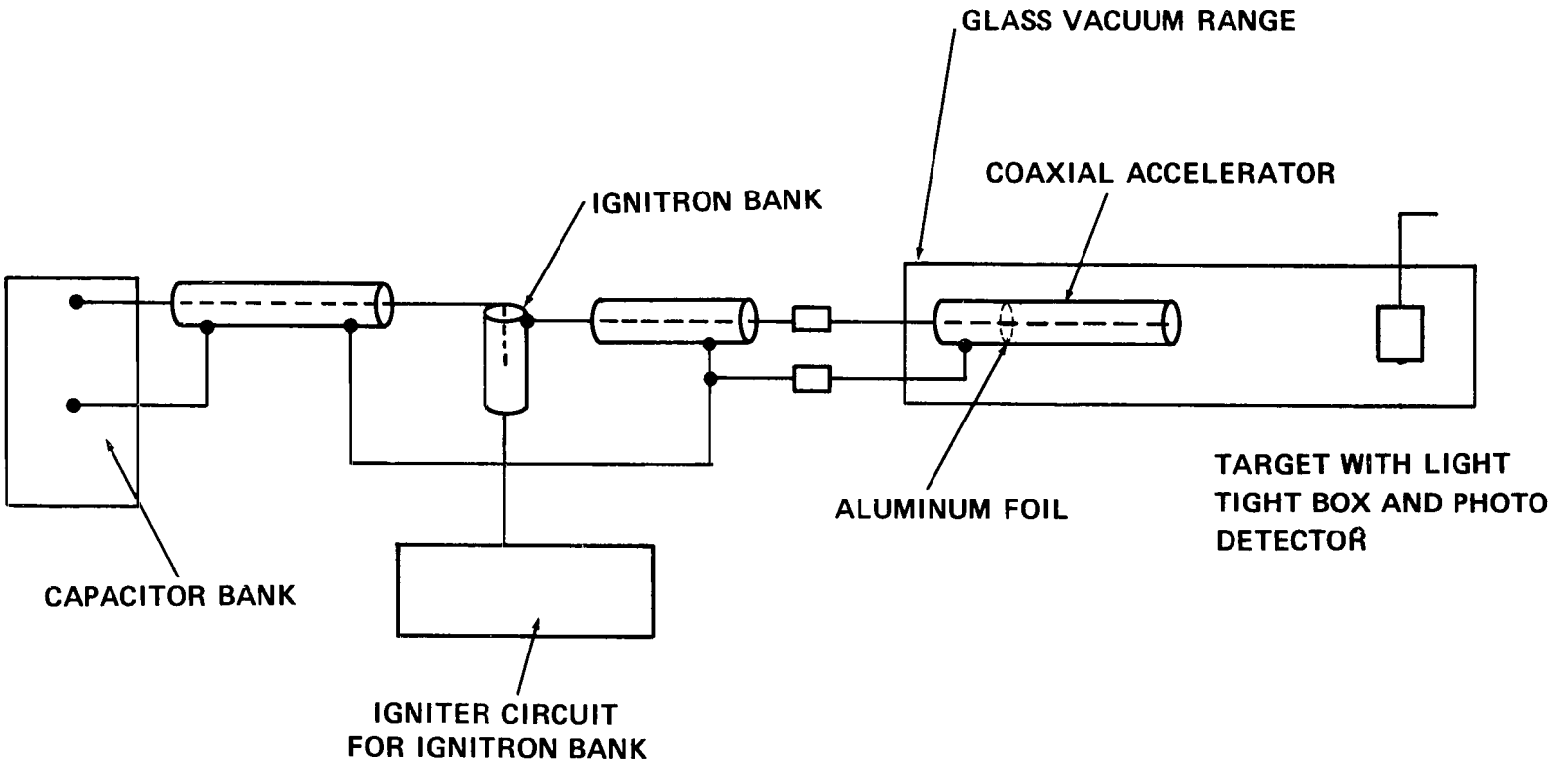

FIGURE 1. SYSTEM SCHEMATIC

with the exception of the coaxial plasma gun which was made of materials readily available commercially and assembled in the laboratory. The dimensions and physical characteristics of the system components are listed in Table 1.

The coaxial gun was loaded by placing an aluminum foil disc, 0.053975 meter in diameter and 6.35×10^{-6} meters thick, in the barrel of the gun, 16.5 centimeters from the muzzle, so that electrical contact existed between the foil and both the center and outer electrodes of the gun. The gun was mounted in one end of the tubular vacuum range and the diagnostic instrumentation was mounted on the vacuum range.

The capacitor bank was charged from a console which provided a rectified high voltage power supply and a safety-dump circuit which could, if necessary, bleed the charge off the capacitor bank. The capacitor bank was discharged through the coaxial plasma gun by triggering the ignitron bank through a thyratron-actuated trigger circuit.

When the capacitor bank was discharged, an emf was impressed across the foil disc causing it to conduct current, evaporate, and ionize by resistive heating of the conducting foil and colliding of the aluminum atoms. Since there was a magnetic field around the center electrode and since the current in the foil was perpendicular to this field, the charged particles were driven down the barrel of the plasma gun by the $\bar{j} \times \bar{B}$ forces. This mechanism produces a very high velocity gas which may be used to accelerate projectiles.

Table 1. Physical Characteristics of Equipment in Coaxial Accelerator Circuit

Equipment/Characteristic	Description
Capacitors	
Peak dc Voltage Rating	20 kilovolt
Capacitance	15 microfarad +20% -10%
Inductance	40 nanohenry max
Energy	300 joule
Voltage Reversal	90%
Peak Current	2×10^5 ampere (direct short)
Life Expectancy	10^5 discharges
Cables	
Type	20 P 2
Peak Voltage	20 kilovolt
Reversal Level for Full Nominal Life	19 kilovolt
Nominal Life	10^5 pulses
Characteristic Impedance	16 ohms ± 1 ohm
Inductance (at 200 kHz)	105 ± 6.6 nanohenry/meter
Delay	6.56 nanosecond/meter
Normal dc Resistance	
Inner Conductor	0.568 ohm/kilometer
Outer Conductor	3.335 ohm/kilometer
Minimum Bending Radius	12.7 centimeter
Capacitance	407 picofarad/meter
Ignitrons	
Type	GL-7703
Peak Anode Voltage (Forward)	20 kilovolt
Peak Ancde Voltage (Reverse)	20 kilovolt
Peak Anode Current for One-Half-Cycle of 20 microsecond	10^5 ampere
Tube Inductance	4×10^{-8} henry
Ionization Time	0.5 microsecond
Ignitor Ratings	
Ignitor Voltage	
Forward Open Circuit	1500 volts min 3000 volts max
Inverse Voltage	5 volts max
Peak Ignitor Current	250 ampere max 200 ampere min
Length of Firing Pulse, Sine Wave	5 microsecond min 10 microsecond max

Circuit Constant Determination

The capacitance, inductance, and resistance of the circuit must be known before any calculation can be made. Since the capacitance of the bank was known and was orders of magnitude higher than any of the capacitances of either the coaxial cables or the gun, which were in parallel with the bank, the capacitance of the circuit was considered to be that of the capacitor bank.

This was not the case for the circuit inductance, however, since the capacitor bank was very low in inductance compared to the other elements of the circuit. The inductance contributed by circuit components of coaxial configuration may be calculated (Appendix A), but the inductance of the ignitrons and the terminal connections must be calculated from ring frequency measurements of the circuit (Appendix B and Fig. 2) where

$$f_o = \frac{1}{2\pi}\sqrt{\frac{1}{L_o C} - \frac{R_o^2}{4L_o^2}} = 13\ 172 \text{ hertz} \quad .$$

Also, by measuring the current amplitude in the ringing circuit, the circuit resistance may be calculated from the expression (Appendix B):

$$\ln \frac{i'_o}{i''_o} = \frac{2\pi \frac{R}{2L_o}}{\sqrt{\frac{1}{L_o C} - \frac{R_o^2}{4L_o^2}}} \quad .$$

The current curve was obtained by placing a test coil of a few turns of wire near the leads from the ignitron bank. [No attempt was made to calibrate the current response since a known current of sufficient strength for

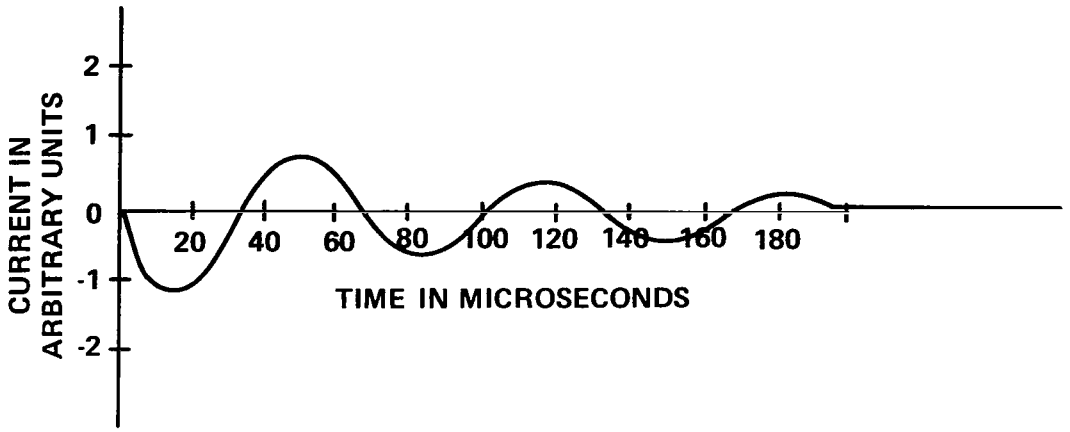

FIGURE 2. RINGING FREQUENCY CURRENT VERSUS TIME

calibration was not available. However, the frequency and relative amplitudes of the current peaks can be obtained from the current curve (Fig. 2).] A short circuit was introducted across the plasma gun, and a voltage of 3000 volts was impressed across the capacitor bank. The bank was then discharged and the circuit underwent a damped oscillating discharge.

The ringing frequency from this curve was determined (Appendix B) by measuring the time interval between zero crossings on the curve. This gives the half period: $T_o = \frac{1}{2f_o}$.

Thus, the frequency, capacitance, inductance, and resistance of the circuit were determined:

f_o = 13 172 hertz (Ringing frequency without accelerator)

C = 270 microfarads (Circuit capacitance without accelerator)

L_o = 0.4157 microhenry (Circuit inductance without accelerator)

R_o = 6.881×10^{-3} ohms (Circuit resistance without accelerator)

Since the plasma gun was only a section of coaxial transmission line for the current-carrying portion, the inductance may be calculated:

$$\lambda = \frac{\mu_o}{2\pi} \ln \frac{b}{a} \text{ henry/meter}$$

$$\lambda = 2 \times 10^{-7} \ln \frac{3.8}{0.635}$$

$$\lambda = 0.3578 \text{ microhenry/meter (accelerator inductance)}$$

Also, the resistance of the gun was measured and was found to be 0.003 ohm. The gun was 0.67 meter long, giving a value of $R_1 = 0.00448$ ohm/meter.

CHAPTER II

THEORY OF THE COAXIAL PLASMA ACCELERATOR

Development of the Circuit Equations

When the aluminum disc was inserted into the gun and the capacitor bank was discharged through the circuit, the discharge was not simply a damped periodic oscillation. The motion of the plasma down the gun barrel caused the current-carrying length of the gun to vary, thereby changing the circuit inductance and resistance.

The equivalent circuit is shown in Figure 3. It can be seen that the circuit consists of fixed capacitance C, fixed inductance L_o, and fixed resistance R_o, all in series with a varying inductance λx and a varying resistance $R_1 x$.

The potential drops around the circuit are given by Kirchoff's law [2]:

$$\frac{d}{dt}\left[(L_o + \lambda x) I\right] + (R_o + R_1 x) I + V_T - V = 0 \quad , \tag{1}$$

where V_T is the potential drop across the plasma caused by the energy loss which is used to heat the plasma, $\frac{d}{dt}\left[(L_o + \lambda x) I\right]$ represents the potential across the inductors, and V is the potential across the capacitor.

$$V = V_o - \frac{1}{C}\int_0^t I\, dt \quad . \tag{2}$$

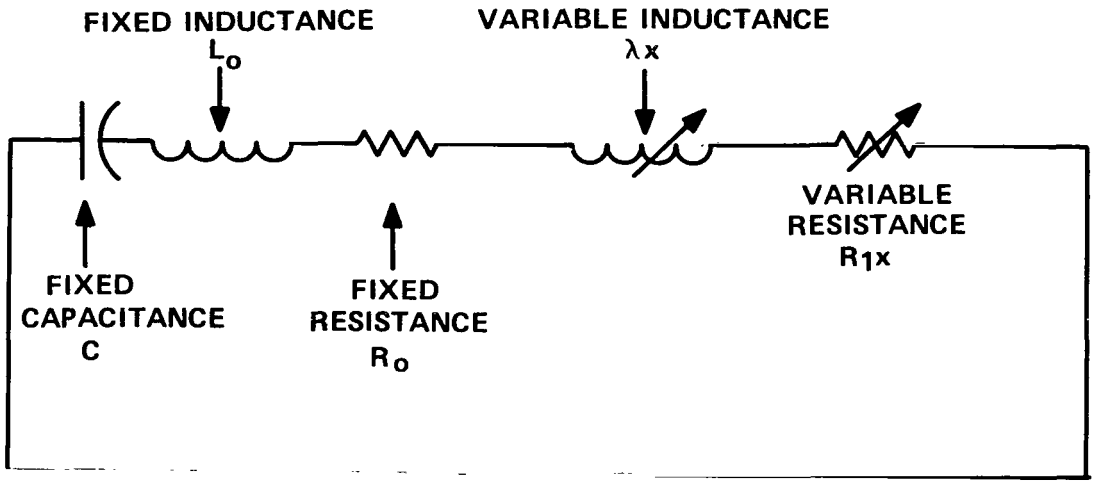

FIGURE 3. SCHEMATIC EQUIVALENT CIRCUIT

After differentiation, equation (1) becomes

$$(L_o + \lambda x)\left(\frac{dI}{dt}\right) + \left[R_o + R_1 x + \lambda \frac{dx}{dt}\right] I + V_T - V = 0 \quad . \qquad (3)$$

The energy balance may be expressed as

$$\frac{1}{2} CV_o^2 = \frac{1}{2} m\left(\frac{dx}{dt}\right)^2 + \frac{1}{2} (L_o + \lambda x) I^2 + \int_0^t (R_o + R_1 x) I^2 \, dt$$

$$+ \int_0^t V_T \, I \, dt + \frac{1}{2} CV^2 \quad . \qquad (4)$$

The term $\int_0^t V_T I \, dt$ is the time integral of the power absorbed in heating the plasma, and the kinetic energy of the moving plasma is

$$KE = \frac{1}{2} m \left(\frac{dx}{dt}\right)^2 \quad .$$

Differentiating equation (4) with respect to time produces the expression

$$0 = m\left(\frac{d^2x}{dt^2}\right)\left(\frac{dx}{dt}\right) + (L_o + \lambda x)\, I \left(\frac{dI}{dt}\right) + \frac{I^2}{2}\,\lambda\left(\frac{dx}{dt}\right)$$

$$+ (R_o + R_1 x)\, I^2 + V_T I + CV\left(\frac{dV}{dt}\right) \quad .$$

Dividing this expression by I produces a new equation:

$$0 = \frac{m}{I}\left(\frac{d^2x}{dt^2}\right)\left(\frac{dx}{dt}\right) + (L_o + \lambda x)\left(\frac{dI}{dt}\right) + \frac{I}{2}\lambda\left(\frac{dx}{dt}\right)$$

$$+ (R_o + R_1 x)\, I + V_T + \frac{CV}{I}\left(\frac{dV}{dt}\right) \quad ,$$

but from equation (2), $\frac{dV}{dt} = -\frac{I}{C}$ and

$$0 = \frac{m}{I}\left(\frac{d^2x}{dt^2}\right)\left(\frac{dx}{dt}\right) + (L_o + \lambda x)\left(\frac{dI}{dt}\right) + \frac{I}{2}\lambda\left(\frac{dx}{dt}\right)$$

$$+ (R_o + R_1 x)\, I + V_T - V \quad . \qquad (5)$$

Now, substract equation (3) from equation (5) to obtain the following equation:

$$\frac{m}{I}\left(\frac{d^2x}{dt^2}\right)\left(\frac{dx}{dt}\right) - \frac{I}{2}\lambda\left(\frac{dx}{dt}\right) = 0$$

or

$$\frac{d^2x}{dt^2} = \frac{\lambda}{2m}\, I^2 \quad . \qquad (6)$$

If the circuit constants and initial conditions are known, the coupled set of equations (3) and (6) may be solved simultaneously to obtain the potential drop across the capacitor, the plasma velocity, and the current. The two equations are

$$\frac{d^2x}{dt^2} = \frac{\lambda}{2m} I^2 \quad ,$$

and

$$(L_o + \lambda x) \frac{dI}{dt} + \left[R_o + R_1 x + \lambda\left(\frac{dx}{dt}\right)\right] I + V_T - V = 0 \quad .$$

These equations, without the resistance terms or plasma heating term, have been solved by others [3, 4, 5] using dimensionless variables. The dimensionless set of equations was

$$\frac{d^2\xi}{d\tau^2} = k\, i^2$$

and

$$1 - \int i\, d\tau = i \frac{d\xi}{d\tau} + \xi \frac{di}{d\tau} \quad ,$$

where the constant $k = \dfrac{C^2 V_o^{\,2} \lambda}{2ms}$ (s is an equivalent distance) and $L_o + \lambda x_o = \lambda s$ (x_o is the length of the gun barrel on the capacitor side of the aluminum disc). It was found that a value of $k = 1$ most nearly fits the observed discharge conditions. Using this value for k and solving for m, it was found that the mass of the accelerated plasma is

$$m = \frac{C^2 V_o^{\,2} \lambda^2}{2(L_o + \lambda x_o)} \quad . \tag{7}$$

Substituting this mass expression into equation (6), the differential equation becomes

$$\frac{d^2x}{dt^2} = \left(\frac{L_o + \lambda x_o}{C^2 V_o^{\,2} \lambda}\right) I^2 \quad .$$

To solve the coupled set of equations, the voltage arising from the resistance of the plasma, V_T, must be expressed as an analytic function of the current.

If it is assumed that the resistivity of aluminum remains constant during the heating and ionization process, the voltage across the foil can be calculated. The resistivity of the aluminum at the melting point is [6]:

$$\rho = 10.7 \times 10^{-6} \text{ ohm - cm} \quad .$$

The resistivity is a nearly linear function of the temperature throughout the solid phase, but no information is available for the liquid phase. In any case, the resistivity will probably not change by orders of magnitude as long as the density remains constant. Then, the resistance of the aluminum disc can be calculated where the resistance is

$$R_2 = \rho \frac{l}{A} \quad ,$$

l is the conductor length and A is the cross-sectional area of the conductor.

For a conductor of annular cross section of length l, thickness da, and radius a, the resistance is (Fig. 4):

$$dR_2 = \rho \frac{da}{2\pi l a}$$

and

$$R_2 = \frac{\rho}{2\pi l} \ln \frac{a_{max}}{a_{min}} \quad .$$

Then, for the disc used, $R_2 = 4.798 \times 10^{-3}$ ohms.

The voltage drop across the disc will then be

$$V_T = I R_2 \quad .$$

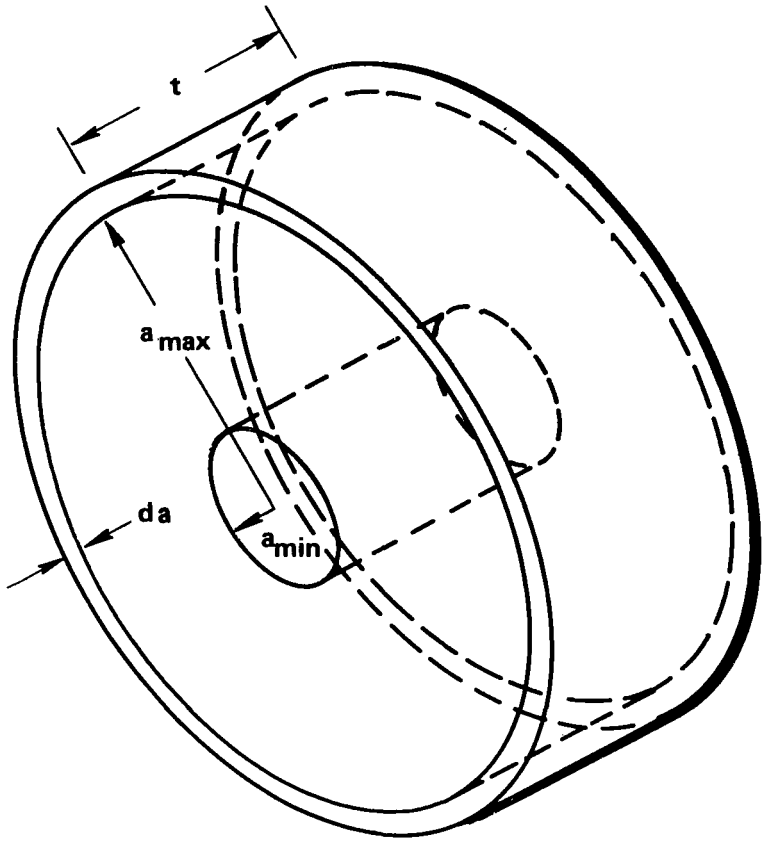

FIGURE 4. RESISTANCE ELEMENT OF A DISC CONDUCTOR

The differential equations then become

$$(L_o + \lambda x)\frac{d^2V}{dt^2} + \left[R_o + R_1 x + R_2 + \lambda\left(\frac{dx}{dt}\right)\right]\frac{dV}{dt} + \frac{V}{C} = 0 \quad .$$

and

$$\frac{d^2x}{dt^2} = \frac{L_o + \lambda x_o}{V_o{}^2\lambda}\left(\frac{dV}{dt}\right)^2 \quad ,$$

after substituting for V_T, I, and $\frac{dI}{dt}$.

Solution of the Circuit Equations

These equations were solved on the Sperry-Rand 1108 computer using a fourth-order Runge-Kutta program. When solving the equations, the

simultaneous solution was used until the value of x was equal to the length of the gun barrel. At this time, only the damped oscillator solution is applicable, since $\frac{dx}{dt}$ is constant and $\frac{d^2x}{dt^2} = 0$. The following set of initial conditions was used (at time $t = 0$) (Appendix C):

$$x = x_o = 0.505 \text{ meter}$$

$$V = V_o = 1.6 \times 10^4 \text{ volts}$$

$$L_o = 4.157 \times 10^{-7} \text{ henrys}$$

$$\lambda = 3.578 \times 10^{-7} \text{ henrys/meter}$$

$$R_o = 6.881 \times 10^{-3} \text{ ohms}$$

$$R_1 = 4.48 \times 10^{-3} \text{ ohms}$$

$$R_2 = 4.798 \times 10^{-3} \text{ ohms}$$

$$C = 2.7 \times 10^{-4} \text{ farads}$$

$$\frac{dx}{dt} = 0$$

$$\frac{d^2x}{dt^2} = 0$$

CHAPTER III

THE LOW-FREQUENCY MAGNETIC FIELDS IN A DISC ARISING FROM RADIAL CURRENTS

Development of the Expression for the Magnetic Field

In a metallic disc conductor with free charge, where the permeability, μ, and conductivity, σ, are isotropic and not time-dependent, Maxwell's equations are

$$\bar{\nabla} \cdot \bar{D} = \rho \quad , \tag{8}$$

$$\bar{\nabla} \cdot \bar{B} = 0 \quad , \tag{9}$$

$$\bar{\nabla} \times \bar{E} = -\mu \frac{\partial \bar{H}}{\partial t} \quad , \tag{10}$$

and

$$\bar{\nabla} \times \bar{B} = \mu \bar{j} + \mu \frac{\partial \bar{D}}{\partial t} \quad . \tag{11}$$

The curl of equation (10) is

$$\bar{\nabla} \times (\bar{\nabla} \times \bar{E}) = -\mu \frac{\partial}{\partial t} (\bar{\nabla} \times \bar{H}) \tag{12}$$

or

$$\bar{\nabla} \times (\bar{\nabla} \times \bar{E}) = -\mu \frac{\partial}{\partial t} \left(\sigma \bar{E} + \epsilon \frac{\partial \bar{E}}{\partial t} \right) \quad ,$$

since $\bar{D} = \epsilon \bar{E}$, and, by Ohm's law, $\bar{j} = \sigma \bar{E}$, so that

$$\bar{\nabla} \times (\bar{\nabla} \times \bar{E}) = - \sigma \mu \frac{\partial \bar{E}}{\partial t} - \epsilon \mu \frac{\partial^2 E}{\partial t^2} \qquad (13)$$

Now, for a time periodic field where

$$E (q_k, t) = E (q_k) (\exp i \omega t) \quad ,$$

and q_k is a set of orthogonal space coordinates,

$$\bar{\nabla} \times [\bar{\nabla} \times \bar{E} (q_k)] (\exp i \omega t) = - i \sigma \mu \omega \bar{E} (q_k) (\exp i \omega t)$$

$$+ \epsilon \mu \omega^2 \bar{E} (q_k) (\exp i \omega t)$$

or

$$\bar{\nabla} \times (\bar{\nabla} \times \bar{E}) = \left(1 - \frac{i \sigma}{\epsilon \omega}\right) \mu \epsilon \omega^2 \bar{E} \quad . \qquad (14)$$

For aluminum,

$\sigma = 3.5 \times 10^7$ mho/meter ,

$\mu = \mu_o$ (approximately) $= 4\pi \times 10^{-7}$ henry/meter ,

and

$\epsilon = \epsilon_o$ (approximately) $= \frac{1}{36\pi} \times 10^{-9}$ farad/meter .

Then, the imaginary term in equation (14) has a coefficient

$$\frac{\sigma}{\epsilon \omega} = \frac{4.56 \times 10^{18}}{\omega} \quad \text{(approximately)} \quad .$$

This term is very large compared to unity except for extremely high frequencies; therefore, the displacement term, which is real, can be ignored at low frequencies.

Under these conditions, Maxwell's equations become

$$\bar{\nabla} \cdot \bar{E} = 0 \quad , \qquad (15)$$

$$\bar{\nabla} \cdot \bar{B} = 0 \quad , \qquad (16)$$

$$\bar{\nabla} \times \bar{E} = - \frac{\partial \bar{B}}{\partial t} \quad , \tag{17}$$

$$\bar{\nabla} \times \bar{B} = \mu \bar{j} \quad . \tag{18}$$

Equation (18) is sometimes referred to as Ampere's law.

Now consider a disc and let a set of cylindrical coordinates R, Θ, Z, be situated with the origin at the center of the disc and the Z axis perpendicular to the plane of the disc (Fig. 5).

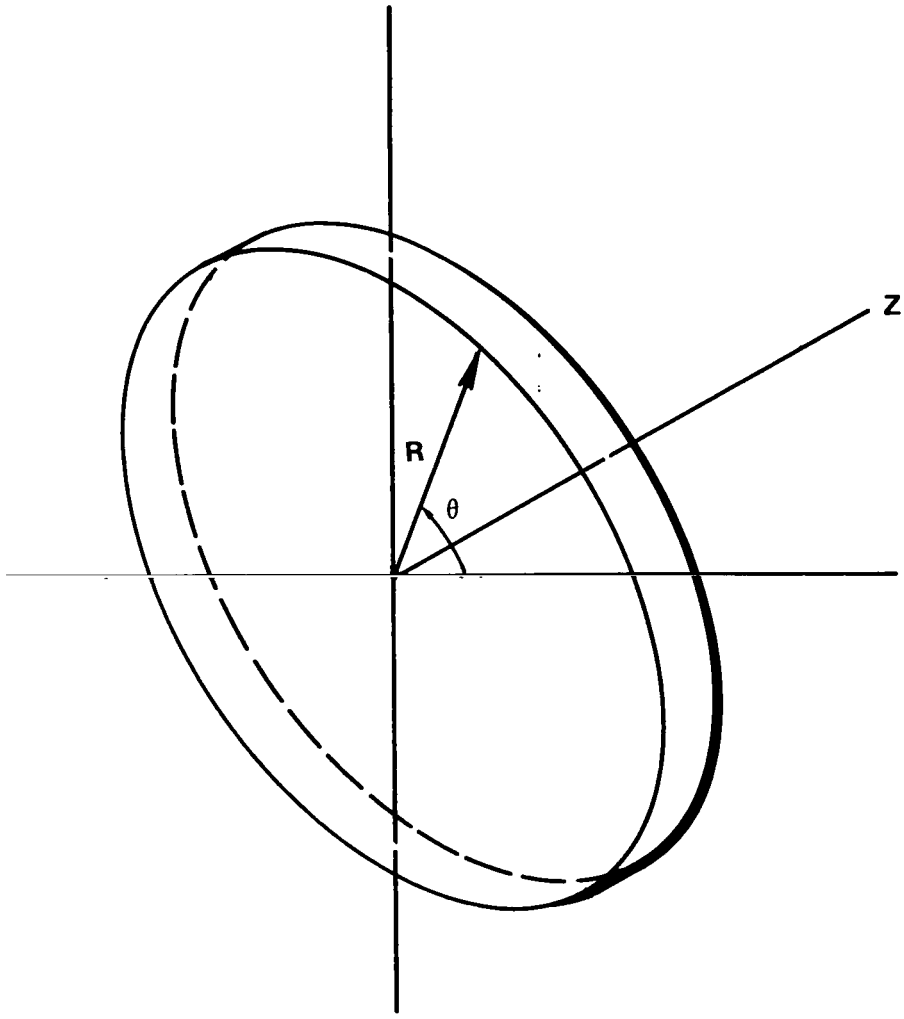

FIGURE 5. CYLINDRICAL COORDINATES OF A CIRCULAR CYLINDRICAL DISC

In an orthogonal coordinate system, the curl of any vector [7] $\overline{F}$ is

$$\overline{\nabla} \times \overline{F} = \frac{\hat{a}_1}{h_2 h_3} \left[\frac{\partial}{\partial q_2} (h_3 F_3) - \frac{\partial}{\partial q_3} (h_2 F_2) \right]$$

$$+ \frac{\hat{a}_2}{h_3 h_1} \left[\frac{\partial}{\partial q_3} (h_1 F_1) - \frac{\partial}{\partial q_1} (h_3 F_3) \right]$$

$$+ \frac{\hat{a}_3}{h_1 h_2} \left[\frac{\partial}{\partial q_1} (h_2 F_2) - \frac{\partial}{\partial q_2} (h_1 F_1) \right] .$$

The divergence is

$$\overline{\nabla} \cdot \overline{F} = \frac{1}{h_1 h_2 h_3} \left[\frac{\partial}{\partial q_1} (F_1 h_2 h_3) + \frac{\partial}{\partial q_2} (h_1 F_2 h_3) + \frac{\partial}{\partial q_3} (h_1 h_2 F_3) \right].$$

In a cylindrical coordinate system, the square of the elemental distance element is

$$ds^2 = dR^2 + R^2 d\theta^2 + dz^2 \quad , \tag{19}$$

and the scale factors are $h_1 = 1$, $h_2 = R$, and $h_3 = 1$. Now let $R = r + r_o$ so that $dR = dr$, then

$$ds^2 = dr^2 + (r + r_o)^2 d\theta^2 + dz^2 \quad , \tag{20}$$

and $h_1 = 1$, $h_2 = r + r_o$, and $h_3 = 1$.

The curl then becomes

$$\overline{\nabla} \times \overline{F} = \frac{\hat{r}}{r + r_o} \left[\frac{\partial F_z}{\partial \theta} - \frac{\partial (r + r_o) F_\theta}{\partial z} \right] + \hat{\theta} \left[\frac{\partial F_r}{\partial z} - \frac{\partial F_z}{\partial r} \right]$$

$$+ \frac{\hat{z}}{r + r_o} \left[\frac{\partial (r + r_o) F_\theta}{\partial \theta} - \frac{\partial F_r}{\partial \theta} \right] ,$$

and the divergence becomes

$$\bar{\nabla} \cdot \bar{F} = \frac{1}{r + r_o} \frac{\partial (r + r_o) F_r}{\partial r} + \frac{1}{r + r_o} \frac{\partial F_\theta}{\partial \theta} + \frac{\partial F_z}{\partial z} \quad .$$

In the case of a disc with a slowly varying time periodic electric field applied in the radial direction, the components of the vectors in Ampere's law, equation (18), are

$$\frac{1}{r + r_o} \frac{\partial B_z}{\partial \theta} - \frac{\partial B_\theta}{\partial \theta} = \mu j_r \quad , \tag{21}$$

$$\frac{\partial B_r}{\partial z} - \frac{\partial B_z}{\partial r} = 0 \quad , \tag{22}$$

and

$$\frac{1}{r + r_o} \frac{\partial (r + r_o) B_\theta}{\partial r} - \frac{1}{r + r_o} \frac{\partial B_r}{\partial \theta} = 0 \quad . \tag{23}$$

The divergence of $\bar{B}$ is

$$\frac{1}{r + r_o} \frac{\partial (r + r_o) B_r}{\partial r} + \frac{1}{r + r_o} \frac{\partial B_\theta}{\partial \theta} + \frac{\partial B_z}{\partial z} = 0 \quad . \tag{24}$$

(The time periodicity in these equations is not written but is assumed to be present.)

Since the disc is symmetric about the Z axis, there is no θ dependence, and

$\bar{B} \neq \bar{B}(\theta)$ and $\bar{E} \neq \bar{E}(\theta)$.

From Ohm's law, $\bar{j} = \sigma \bar{E}$ for the disc; therefore, if the only nonzero component of $\bar{j}$ is in the r direction,

$$\bar{\nabla} \times \bar{B} = \mu j_r \hat{r} \quad .$$

From equation (17), the curl of the electric field is

$$\bar{\nabla} \times \bar{E} = - \frac{\partial \bar{B}}{\partial t} \quad ,$$

and since $\bar{E} = E_r \hat{r}$,

$$\bar{\nabla} \times \bar{E} = \bar{\nabla} \times E_r \hat{r} = \hat{\theta} \frac{1}{r} \frac{\partial (r E_r)}{\partial z} = - \frac{\partial \bar{B}}{\partial t}$$

and

$$B_r = B_z = 0$$

since $\bar{B}$ has only a θ component.

Then

$$\frac{\partial E_r}{\partial z} = - \frac{\partial B_\theta}{\partial t} \quad . \tag{25}$$

After differentiating,

$$\frac{\partial^2 E_r}{\partial z^2} = - \frac{\partial}{\partial t} \frac{\partial B_\theta}{\partial z} = \frac{\partial}{\partial t} (\mu j_r)$$

from equation (21).

From Ohm's law $j_r = \sigma E_r$, so that

$$\frac{\partial^2 E_r}{\partial z^2} = \frac{\partial}{\partial t} (\sigma \mu E_r) \quad . \tag{26}$$

The field is applied in the radial direction so that

$$E_r(R, z, t) = E_r(R, z)\ (\exp i\omega t); \tag{27}$$

then

$$\frac{\partial^2 E_r}{\partial z^2} = i\omega\sigma\mu E_r(R, z)\ (\exp i\omega t) \quad .$$

From equation (15),

$$\bar{\nabla} \cdot \bar{E} = 0 \quad ,$$

or

$$\frac{1}{R} \frac{\partial (RE_r)}{\partial R} = 0 \quad ,$$

and, from equation (27),

$$\frac{1}{R} \frac{\partial}{\partial R} [R\sigma\mu E_r(R, z)\ (\exp i\omega t)] = 0 \quad .$$

This implies that

$$RE_r(R,z) = g(z)(\exp i\omega t) \quad . \tag{28}$$

The function $g(z)$ must be an even function since the electric field must have the same magnitude on both sides of the disc.

$$g(z) = g(-z) \quad .$$

The maximum electric field on the disc occurs when $\exp i\omega t = 1$, and when the variables R and z have the values

$$R = r_o$$

$$z = \pm z_{max}$$

The function $g(z)$ will then have the value

$$g(z_{max}) = r_o E_{or} \quad .$$

Then, from equation (28),

$$E_r(R, z, t) = \frac{g(z)}{R} (\exp i \omega t) \quad . \tag{29}$$

It has been shown that

$$\frac{\partial^2 E_r}{\partial z^2} = \frac{\partial}{\partial t} (\sigma \mu E_r) \quad ;$$

so

$$\frac{\partial^2 E_r}{\partial z^2} = \frac{1}{R} \frac{\partial}{\partial z} \left[\frac{dg(z)}{dz} \right] (\exp i \omega t) = \frac{1}{R} \frac{d^2 g(z)}{dz^2} (\exp i \omega t)$$

and

$$\frac{\partial}{\partial t} (\sigma \mu E_r) = \frac{i \omega \sigma \mu}{R} g(z) (\exp i \omega t) \quad .$$

Then

$$\frac{d^2 g(z)}{dz^2} = i \omega \sigma \mu g(z)$$

and

$$(D^2 - i \omega \sigma \mu) g(z) = 0 \quad . \tag{30}$$

This equation has a solution of the form

$$g(z) = C_1 (\exp \sqrt{i \omega \sigma \mu}\, z) + C_2 \left[\exp \left(- \sqrt{i \omega \sigma \mu}\, z \right) \right] \quad .$$

Since the function $g(z)$ is an even function,

$$g(z) = g(-z)$$

and

$$C_1 = C_2 \quad ,$$

then $g(z)$ will have the form

$$g(z) = C_1 \left\{ (\exp \sqrt{i \omega \sigma \mu}\, z) + \left[\exp \left(-\sqrt{i \omega \sigma \mu} \right) z \right] \right\} \quad .$$

At

$$z = \pm z_{max} \quad , \quad g(z_{max}) = r_o E_{or}$$

so that

$$C_1 = \frac{r_o E_{or}}{\exp \sqrt{i\omega\sigma\mu}\, z_{max} + \exp\left(-\sqrt{i\omega\sigma\mu}\right) z_{max}} \tag{31}$$

or

$$g(z) = r_o E_{or} \left\{\left(\exp\sqrt{i\omega\sigma\mu}\, z\right) + \left[\exp\left(-\sqrt{i\omega\sigma\mu}\right) z\right]\right\}$$
$$\div \left\{\left(\exp\sqrt{i\omega\sigma\mu}\, z_{max}\right) + \left[\exp\left(-\sqrt{i\omega\sigma\mu}\right) z_{max}\right]\right\} .$$

Since $i = \exp \frac{i\pi}{2}$,

$$\sqrt{i} = \exp \frac{i\pi}{4} = \cos \frac{\pi}{4} + i \sin \frac{\pi}{4} = \frac{\sqrt{2}}{2} (1 + i) \quad ,$$

then

$$g(z) = r_o E_{or} \left(\exp \frac{\sqrt{2\sigma\mu\omega}}{2} z\right)\left(\exp \frac{i\sqrt{2\sigma\mu\omega}}{2} z\right)$$
$$+ \left[\exp\left(-\frac{\sqrt{2\sigma\mu\omega}}{2}\right) z\right]\left[\exp\left(-\frac{i\sqrt{2\sigma\mu\omega}}{2}\right) z\right] .$$
$$\div \left\{\left(\exp \frac{\sqrt{2\sigma\mu\omega}}{2} z_{max}\right)\left(\exp \frac{i\sqrt{2\sigma\mu\omega}}{2} z_{max}\right)\right.$$
$$\left. + \left[\exp\left(-\frac{\sqrt{2\sigma\mu\omega}}{2}\right) z_{max}\right]\left[\exp\left(-\frac{i\sqrt{2\sigma\mu\omega}}{2}\right) z_{max}\right]\right\} .$$

After expanding, and letting the second term be A ,

$$g(z) = r_o E_{or} \left[\left(i \cos \frac{\sqrt{2\sigma\mu\omega}}{2} z - \sin \frac{\sqrt{2\sigma\mu\omega}}{2} z \right) \left(\cos \frac{\sqrt{2\sigma\mu\omega}}{2} z + i \sin \frac{\sqrt{2\sigma\mu\omega}}{2} z \right) + \left(i \cos \frac{\sqrt{2\sigma\mu\omega}}{2} z + \sin \frac{\sqrt{2\sigma\mu\omega}}{2} z \right) \times \left(\cos \frac{\sqrt{2\sigma\mu\omega}}{2} z - i \sin \frac{\sqrt{2\sigma\mu\omega}}{2} z \right) \right] \div A \quad ,$$

or collecting terms and writing out A ,

$$g(z) = r_o E_{or} \left(\cos^2 \frac{\sqrt{2\sigma\mu\omega}}{2} z - \sin^2 \frac{\sqrt{2\sigma\mu\omega}}{2} z \right) \div \left(\cos^2 \frac{\sqrt{2\sigma\mu\omega}}{2} z_{max} - \sin^2 \frac{\sqrt{2\sigma\mu\omega}}{2} z_{max} \right) \quad .$$

z_{max} is the largest z dimension of the disc and is equal to 3.175×10^{-6} meters. For aluminum, $\sigma\mu = 44$ (approximately); then, for a frequency of 13 172 hertz, $\frac{\sqrt{2\sigma\mu\omega}}{2} = 5.38 \times 10^2$.

Under these conditions, $\sin \frac{\sqrt{2\sigma\mu\omega}}{2} z = 0$ and $\cos \frac{\sqrt{\sigma\mu\omega}}{2} z = 1$ approximately. Therefore, g(z) is constant over the dimensions of the disc and the skin effect may be neglected at this frequency.

It has been shown that

$$E_r(R, z, t) = \frac{g(z)}{R} \exp i\omega t$$

and

$$\overline{\nabla} \cdot \overline{B} = 0 \quad ,$$

so that

$$\frac{1}{R}\,\frac{\partial}{\partial R}\,(R\,B_\theta) = 0$$

from equation (24).

Then $RB_\theta = f(z,t) + C$, at most.

From equation (25),

$$-\frac{\partial B_\theta}{\partial t} = -\frac{1}{R}\,\frac{\partial}{\partial t}\,(f(z,t) + C) = -\frac{1}{R}\,\frac{\partial}{\partial t}\,f(z,t) \qquad . \qquad (32)$$

Then,

$$\frac{\partial E_r}{\partial z} = \frac{1}{R}\,\frac{dg(z)}{dz}\,(\exp i\omega t) = -\frac{1}{R}\,\frac{\partial}{\partial t}\,f(z,t) \quad ,$$

$$\int \frac{\partial}{\partial t}\,f(z,t)\,dt = -\frac{dg(z)}{dz}\int (\exp i\omega t)\,dt \quad ,$$

$$f(z,t) = \frac{i}{\omega}\,\frac{dg(z)}{dz}\,(\exp i\omega t) + C \quad ,$$

$$B_\theta = \frac{i}{\omega R}\,\frac{dg(z)}{dz}\,(\exp i\omega t) + C \quad ,$$

and

$$B_\theta = \frac{1}{\omega R}\,\frac{dg(z)}{dz}\left[\exp i\left(\omega t + \frac{\pi}{2} + C'\right)\right] \qquad . \qquad (33)$$

From equation (21) and Ohm's law,

$$\frac{\partial B_\theta}{\partial z} = -\sigma\mu E_r$$

and

$$\frac{\partial B_\theta}{\partial z} = \frac{1}{\omega R}\,\frac{d^2g(z)}{dz^2}\left[\exp i\left(\omega t + \frac{\pi}{2} + C'\right)\right] \qquad .$$

Now,

$$g(z) = r_o E_{or} \left(\cos^2 \frac{\sqrt{2\sigma\mu\omega}}{2} z - \sin^2 \frac{\sqrt{2\sigma\mu\omega}}{2} z \right)$$

$$\div \left(\cos^2 \frac{\sqrt{2\sigma\mu\omega}}{2} z_{max} - \sin^2 \frac{\sqrt{2\sigma\mu\omega}}{2} z_{max} \right) \quad ;$$

$$\frac{dg(z)}{dz} = - r_o E_{or} \left(\sqrt{2\sigma\mu\omega} \sin \frac{\sqrt{2\sigma\mu\omega}}{2} z \cos \frac{\sqrt{2\sigma\mu\omega}}{2} z \right)$$

$$\div \left(\cos^2 \frac{\sqrt{2\sigma\mu\omega}}{2} z_{max} - \sin^2 \frac{\sqrt{2\sigma\mu\omega}}{2} z_{max} \right) \quad ;$$

$$\frac{d^2g(z)}{dz^2} = r_o E_{or} \sigma\mu\omega \left(\cos^2 \frac{\sqrt{2\sigma\mu\omega}}{2} z - \sin^2 \frac{\sqrt{2\sigma\mu\omega}}{2} z \right) \quad ;$$

$$\div \left(\cos^2 \frac{\sqrt{2\sigma\mu\omega}}{2} z_{max} - \sin^2 \frac{\sqrt{2\sigma\mu\omega}}{2} z_{max} \right) \quad ;$$

and

$$\frac{d^2g(z)}{dz^2} = \sigma\mu\omega\, g(z) \quad ; \qquad (34)$$

and by substituting for E_r

$$- \sigma\mu E_r = - \frac{\sigma\mu}{R} g(z) \exp i\omega t \quad .$$

Then

$$- \sigma\mu\, g(z) \exp i\omega t = \sigma\mu\, g(z) \exp i(\omega t + \frac{\pi}{2} + C')$$

and for this condition to be true

$$C' = \frac{\pi}{2} \quad .$$

Then, from equation (33),

$$B_\theta = \left[\frac{r_o E_{or} \sqrt{2\sigma\mu\omega}}{\omega R} \left(\sin \frac{\sqrt{2\sigma\mu\omega}}{2} z \cos \frac{\sqrt{2\sigma\mu\omega}}{2} z \right) \right.$$

$$\left. \div \left(\cos^2 \frac{\sqrt{2\sigma\mu\omega}}{2} z_{max} - \sin^2 \frac{\sqrt{2\sigma\mu\omega}}{2} z_{max} \right) \right] \exp i\omega t \qquad (35)$$

Therefore, the magnetic fields in the disc are in time phase with the electric fields, and, since the cosine is an even function and the sine is an odd function, the direction of the magnetic field reverses between $z = z_{max}$ and $z = -z_{max}$.

The Magnetic and Thermal Pressures on the Disc

The direction of the magnetic fields in the disc are such that if the current flows from the center of the disc to the rim, the field on the disc surface at the muzzle end of the plasma generator will be directed clockwise when viewed from the muzzle. Conversely, the field on the opposing surface will be counterclockwise. Thus, the force on the plasma will be directed into the disc on both sides of the disc.

The magnetic force will be:

$$\bar{j} \times \bar{B} = -\frac{1}{\mu} \bar{B} \times (\bar{\nabla} \times \bar{B}) \quad ,$$

$$\bar{j} \times \bar{B} = -\frac{1}{\mu} \bar{\nabla} \bar{B} \cdot \bar{B} + \frac{1}{\mu} (\bar{B} \cdot \bar{\nabla}) \bar{B} \quad ,$$

$$\bar{j} \times \bar{B} = -\frac{1}{\mu} \frac{\nabla B^2}{2} + \frac{1}{\mu} \bar{B} \cdot \bar{\nabla} \bar{B} \quad . \qquad (36)$$

The term $\frac{B^2}{2\mu}$ is called the magnetic pressure, and the second term can be considered as force directed parallel to the magnetic field [8].

If the gas dynamic pressure exceeds the magnetic pressure, the disc shape of the plasma may be distorted. It has been shown [equation (35)] that

$$B_\theta = \left[\frac{r_o E_{or} \sqrt{2\sigma\mu\omega}}{\omega R} \left(\sin \frac{\sqrt{2\sigma\mu\omega}}{2} z \cos \frac{\sqrt{2\sigma\mu\omega}}{2} z \right) \right.$$

$$\left. \div \left(\cos^2 \frac{\sqrt{2\sigma\mu\omega}}{2} z_{max} - \sin^2 \frac{\sqrt{2\sigma\mu\omega}}{2} z_{max} \right) \right] \exp i\omega t \quad ,$$

and, if,

$$\frac{\sqrt{2\sigma\mu\omega}}{2} z \ll 1 \quad ,$$

then

$$\cos \frac{\sqrt{2\sigma\mu\omega}}{2} z = 1 \text{ and } \sin \frac{\sqrt{2\sigma\mu\omega}}{2} z = \frac{\sqrt{2\sigma\mu\omega}}{2} z \text{ (approximately)}$$

Under these conditions,

$$B_\theta = \frac{\sigma\mu r_o E_{or}}{R} z \exp i\omega t \quad . \tag{37}$$

Since the resistance of the coaxial gun is negligible, it may be considered as a coaxial capacitor made up of the two conductors which are then short-circuited by the aluminum disc. Then, the inner conductor may be considered a line charge. The field outside the radius r_o is given by Gauss' law for a cylinder where

$$\int_S \epsilon_o \bar{E} \cdot d\bar{S} = Q$$

and

$$\epsilon_o E_{or} (2\pi r_o)\ell = Q \quad ,$$

or

$$E_{or} = \frac{Q_L}{2\pi\epsilon_o r_o} \quad ,$$

where Q_L is the charge density per unit length.

Using this value for E_{or} will yield the following equation for magnetic field strength:

$$\overline{B} = \frac{\sigma\mu\ Q_L}{2\pi\epsilon_o R}\ z\ \exp\ i\omega t\ \hat{\theta} \ .$$

Now,

$$\overline{E} = -\overline{\nabla}\ V \quad ,$$

and, for a cylindrical conductor of line charge density Q_L,

$$E_r = \frac{Q_L}{2\pi\epsilon_o R} = -\frac{dV}{dr} \quad ,$$

or

$$V_{R_{max}} - V_{ro} = -\frac{Q_L}{2\pi\epsilon_o} \ln \frac{R_{max}}{r_o}$$

and

$$Q_L = \frac{2\pi\epsilon_o V_{ro}}{\ln \frac{R_{max}}{r_o}}$$

when $V_{R_{max}} = 0$. Then, the magnetic field is

$$B_\theta = \frac{\sigma\mu V_{ro}}{R \ln \frac{R_{max}}{r_o}} z \exp i\omega t \quad .$$

The maximum magnetic field strength will occur when

$$z = z_{max} \quad ,$$

$$R = r_o \quad ,$$

and

$$\exp i\omega t = 1$$

Then, with the voltages and dimensions used in the experiment, the maximum magnetic field will be, assuming the full voltage is applied to the disc,

$$B_\theta(max) = 3.933 \times 10^2 \text{ weber/square meter at } R = r_o$$

and

$$B_\theta(min) = 65.73 \text{ weber/square meter at } R = R_{max}$$

The magnetic pressure term is

$$p_m = 6.16 \times 10^{10} \text{ Newtons/square meter at } R = r_o$$

and

$$p_m = 1.72 \times 10^9 \text{ Newtons/square meter at } R = R_{max}$$

If the neutral gas and plasma were in thermal equilibrium, the disc shape of the plasma might be distorted. There is no evidence of such distortion, and to the contrary the plume leaving the muzzle is pointed as it would be under the influences of the magnetic field arising from current in the center electrode. This behavior is depicted in Fig. 6. The pointed plume is caused by the difference in magnetic pressure near the center electrode and the magnetic pressure near the outer electrode.

The ionized aluminum cannot expand into the accelerator since it is under the influence of the $\bar{j} \times \bar{B}$ forces arising from the magnetic field around the center electrode and the current in the plasma. However, the gaseous aluminum will expand into the accelerator since it is not acted upon by the magnetic field. Also, because of equipment limitations in available vacuum pump speeds, the atmospheric leakage into the range made it impossible to achieve a vacuum below 0.1 Newton/square meter. This much atmosphere within the coaxial gun provides an easy electrical breakdown path between the electrodes. The net result is that instead of the idealized physical situation considered in the development of the theory a much more complex situation actually exists within the plasma gun. After a very short time the gun is filled with electrically conducting gas and acts only as a resistive element in the circuit, except for that portion of the gun which is occupied by the insulating plug (Fig. 7).

FIGURE 6. PLASMA PLUME LEAVING THE MUZZLE OF THE COAXIAL ACCELERATOR

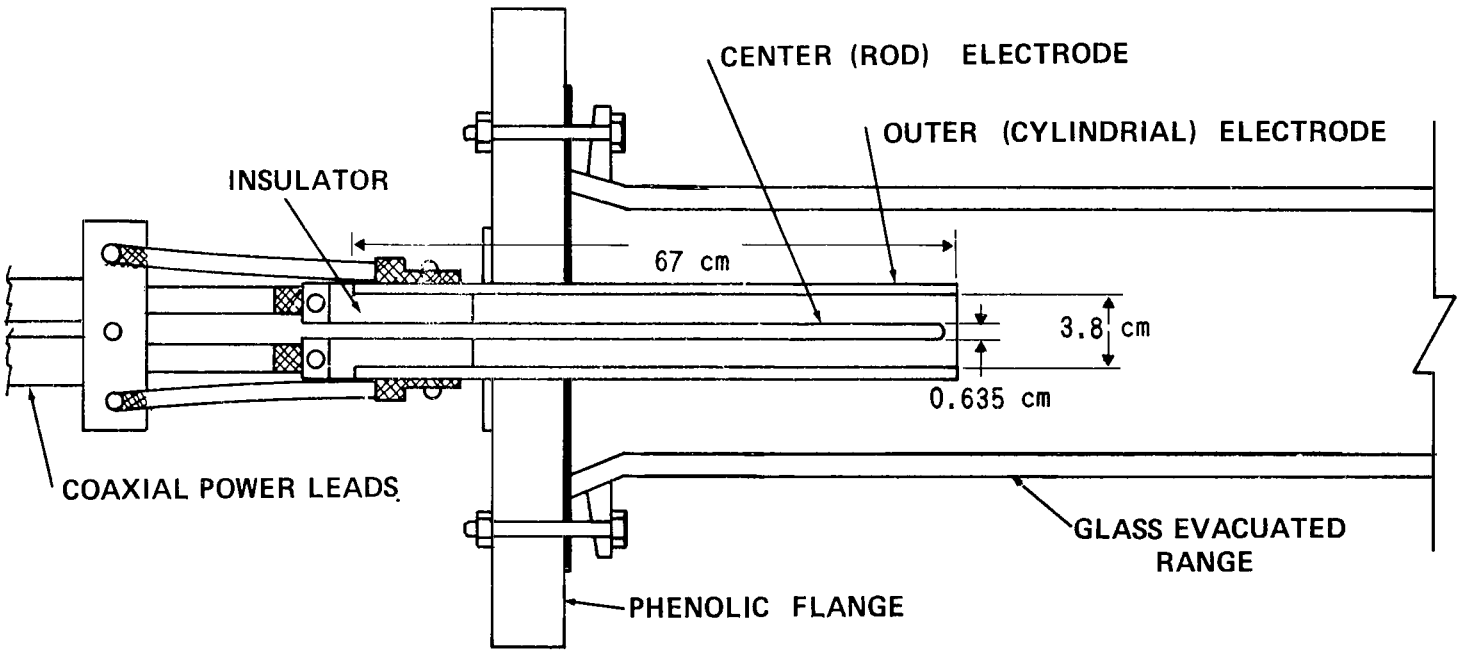

FIGURE 7. COAXIAL PLASMA GENERATOR

CHAPTER IV

DISCREPANCIES BETWEEN THEORETICAL CALCULATIONS AND EXPERIMENTAL RESULTS

By examining Figures 8 and 9 it can be seen that a large frequency discrepancy exists between the calculated current versus time curve and the experimental curve. Also, the difference between the calculated velocities and the velocities obtained experimentally is significant. The simple theory used in the calculations is evidently not sufficient to account for the behavior of the system. Discrepancies have also been noted in the literature [3]. An explanation is offered which may account for the differences between the theory and the experiment.

The aluminum disc used to load the gun weighs 39 milligrams, while the calculated mass of material to be ionized is 2.003 milligrams when a value $k = 1$ is used in the expression

$$m = \frac{V^2 C^2 L_o^2}{2k(L_o + \lambda x_o)} \quad .$$

When the aluminum disc is vaporized, the excess mass expands into the coaxial gun and, because of collision processes between aluminum atoms, provides ions to spread the discharge in a direction opposite to the accelerating

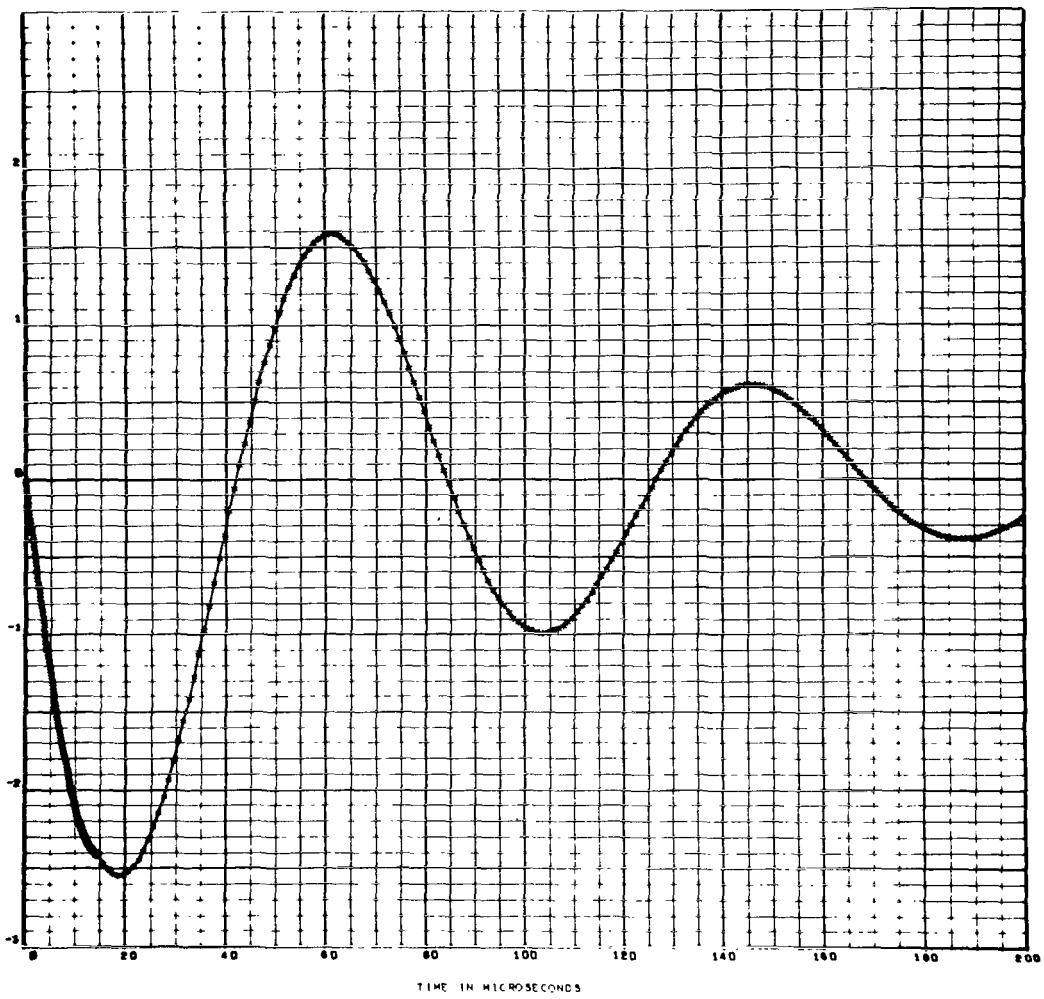

FIGURE 8. THEORETICAL CURRENT VERSUS TIME CURVE

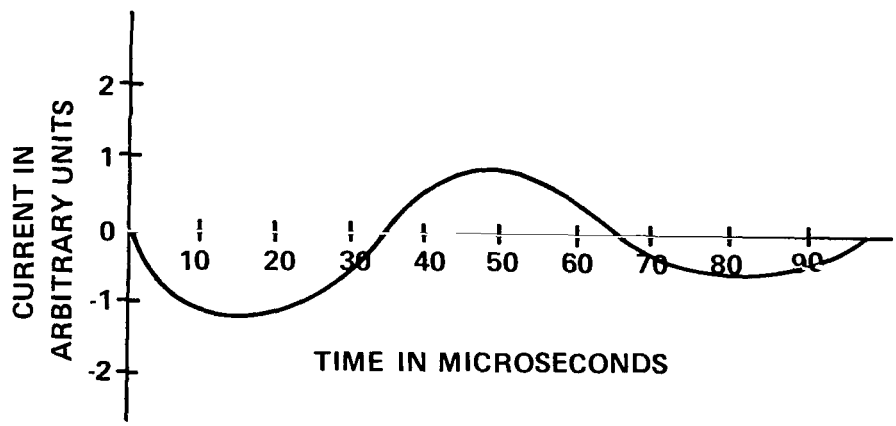

FIGURE 9. CURRENT VERSUS TIME WHEN FIRING COAXIAL GUN

$\bar{j} \times \bar{B}$ forces. To augment this spreading discharge, a considerable amount of atmosphere remains in the gun at a pressure of 0.1 Newton/square meter. This gas is sufficient to cause a breakdown between the gun electrodes when a large difference in potential is applied.

That portion of the coaxial gun which is involved in the discharge now acts as a resistive element in the circuit. Current must still flow in the two electrodes but the current per unit length of electrode is no longer constant. Thus, the magnetic field produced by the current in the inner electrode is changed and the inductance of the circuit approaches the value L_o.

CHAPTER V

THE ENERGY AND MOMENTUM OF THE PLASMA

The Energy Contained in the Plasma

If the previous assumptions are correct, the experimental discharge current curve can be explained. The time interval between the initial current value and the first zero in current is longer than the time interval between succeeding zeroes of current. The time interval between successive zeroes, after the first, agrees with the period of the ringing circuit without the gun.

The mass of the ions accelerated by the magnetic field cannot be obtained from the simple theoretical solution, but must be approximated from one of the three experimental curves for current and velocity. They are the ringing frequency current versus time curve for the circuit without the coaxial gun (Fig. 2), the current versus time curve for the circuit when firing the coaxial gun (Fig. 9), and the distance versus time curve for the advancing plasma plume in the vacuum chamber (Fig. 10).

The equations for current, frequency, and logarithmic decrement shown in Appendix B are

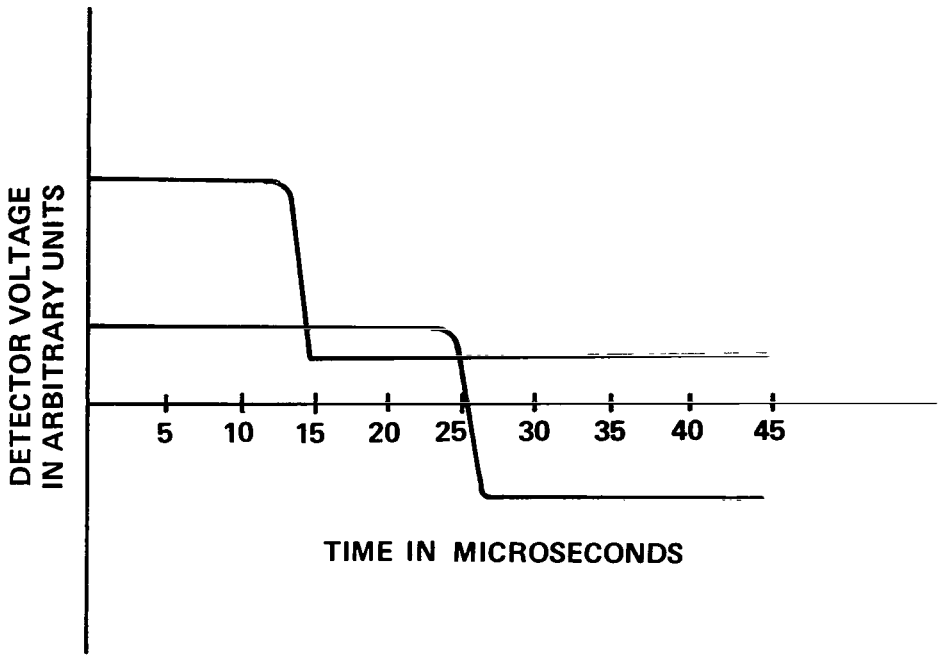

FIGURE 10. DISTANCE VERSUS TIME

$$i = -\left(\frac{\omega_o^2 + \frac{R^2}{4L^2}}{\omega_o}\right) C V_o \left(\exp - \frac{R}{2L} t\right) \sin \omega_o t \quad ,$$

$$f = \frac{1}{2\pi}\sqrt{\frac{1}{LC} - \frac{R^2}{4L^2}} \quad ,$$

and

$$\ln \frac{i'}{i''} = \frac{\frac{\pi R}{2L}}{\sqrt{\frac{1}{LC} - \frac{R^2}{4L^2}}} \quad .$$

The current expression when solved for the current at the first maximum produces an expression which is proportional to the original voltage stored in the capacitor. Without changing any circuit elements, but with a voltage applied in the opposite sense and of a value V_o', the second extrenum in the discharge current curve could be obtained after the same time interval

used in obtaining $i_{1\ max}$. The ratio of the absolute values of the first two current extremums is then equal to the ratio of voltages on the capacitor giving rise to the current extremes.

$$\frac{|i_{1\ max}|}{|i_{2\ max}|} = \frac{V_o}{V'_o} \quad .$$

Then,

$$V'_o = \frac{|i_{2\ max}|}{|i_{1\ max}|} V_o \quad .$$

Since the energy in the capacitor bank is $E = \frac{1}{2} C V^2$, the energies are $E_1 = \frac{1}{2} C V_o^2 = 34.56$ kilojoules and $E_2 = \frac{1}{2} C V_o'^2 = 14.8$ kilojoules. The energy difference between these two is the energy dissipated in the circuit during the first half-cycle of the current discharge curve.

The distributed resistance of the circuit without the coaxial gun has been calculated from the ringing frequency current discharge curve, and the resistance of the coaxial gun was measured using a Wheatstone bridge. The distributed resistance of the circuit, including the coaxial gun, can be calculated from the discharge current curve and is

$$R_T = 1.87 \times 10^{-2} \text{ ohms} \quad .$$

The resistance of the plasma is

$$R_P = R_T - R_o - R_1(0.67)$$

$$R_P = 8.819 \times 10^{-3} \text{ ohms} \quad .$$

Then, the energy dissipated is the plasma is

$$E_P = \Delta E \frac{R_P}{R_T} \quad ,$$

where

$$\Delta E = E_1 - E_2 \quad \text{and} \quad E_P = 9.3 \text{ kilojoules} \quad .$$

By examining Figure 10 it can be seen that the plume front leaves the muzzle of the coaxial gun after 12.5×10^{-6} seconds. A Simpson's rule of integration of the data from the experimental current curve where

$E = \int_o^t I^2 R_P \, dt$ over the first half-cycle of the discharge and over the first 12.5×10^{-6} seconds of discharge can be used to calculate the fraction of the energy absorbed during the first 12.5 microseconds of the first half-cycle.

$$f = \frac{\int_o^{12.5 \times 10^{-6}} I^2 R_P \, dt}{\int_o^{34 \times 10^{-6}} I^2 R_P \, dt} = 0.32 \quad .$$

Then,

$$\Delta E_P = 0.32 \times 9.3 \times 10^3 = 2.98 \times 10^3 \text{ joules} \quad .$$

The fraction of this energy which is actually retained by the aluminum gas is unknown because the heat exchanged between the gun and the electrodes has not been measured or accounted for. There are certain observed phenomena that indicate that a large amount of heat is delivered to the electrodes. For example, after the discharge, the center electrode is

slightly roughened, as though material had been removed, and a noticeable amount of shiny metal, assumed to be aluminum, has been deposited over this. The outer cylindrical electrode is coated on the surface with a grayish black material, assumed to be aluminum oxide. There is no quantitative way of measuring the heat absorbed from the gas. Also, no attempt has been made to distribute the energy among the terms in the energy-balance equation for the partially ionized aluminum gas.

As a first approximation, consider all of the energy absorbed by the plasma as being converted to kinetic energy of the plasma. Then,

$$\frac{1}{2} m v_{av}^2 = E_P \quad .$$

The quantity v_{av}, the average velocity of the plasma, is obtained from Figure 10 which shows the time needed for the plasma plume to travel from the muzzle of the gun to a point 25.4 centimeters downstream.

$$v_{av} = 23 \text{ kilometers/second} \quad .$$

Then,

$$m = \frac{2 \times 2.98 \times 10^3}{(23)^2 \times 10^6} \quad ,$$

$$m = 1.13 \times 10^{-5} \text{ kilogram} \quad ,$$

$$m = 11.3 \text{ milligram} \quad .$$

Since only the ions are accelerated by the magnetic field, and if it is assumed that all of the aluminum is vaporized, the percent ionization is

$$\eta = \frac{11.3}{39} = 29 \text{ percent} \quad .$$

The ions are being accelerated and it is assumed that they fill the gun from the original position of the foil out to the muzzle.

Unquestionably, these values for the energy and mass are too high since the energies of ionization, excitation, particle interaction, degeneracy (Fermi correction), radiation, and plasma oscillation [9,10,11] are not taken into account and the heat lost to the electrodes is ignored.

Transfer of the Plasma Momentum to a Projectile

Since the measured velocity is an average velocity, it will be used to calculate the momentum transfer from the ionized gas to the simulated meteoroid material. It is assumed that the number of ions contained in any cylindrical shell concentric about the center electrode and of radius less than the radius of the outer electrode is constant. This must be true since current is flowing radially between the two electrodes.

Now consider a glass bead 5×10^{-5} meters in diameter to be placed a distance r from the axis of the gun and at the muzzle. Since the difference between the o.d. of the center electrode and the i.d. of the outer electrode is 3.235 centimeters, a total mass of 1.75×10^{-8} kilograms resides in the ring. The mass intercepted by the glass bead will be

$$\Delta m = \frac{\pi\left(\frac{5 \times 10^{-5}}{2}\right)^2 (1.75 \times 10^{-8})}{2\pi r \times 5 \times 10^{-5}} \quad .$$

At the surface of the center electrode, this mass will be

$$\Delta m = 1.72 \times 10^{-11} \text{ kilograms} \quad .$$

This is true assuming a laminar flow so that the geometric cross section of the glass bead may be used in calculating the intercepted mass.

Now, if the collision process between the aluminum ions and the glass bead is elastic so that both linear momentum and kinetic energy are conserved, the velocity of the glass bead may be calculated.

The glass bead has a density of 2.51 and a mass of 1.64×10^{-9} kilograms:

$$(\Delta m)\ v_1 = (\Delta m)\ v_2 + m_G\ V$$

$$\frac{1}{2}(\Delta m)\ v_1^2 = \frac{1}{2}\ (\Delta m)\ v_2^2 + \frac{1}{2}\ m_G\ V^2 \quad .$$

This set of equations must be solved for V, the velocity of the glass bead, when v_1 = 23 kilometers/second:

$$V = 0.48 \text{ kilometer/second} \quad .$$

No provision has been made for the momentum transfer from drag forces between the plasma and the projectile. It has been considered negligible in performing this calculation.

Also the collision process between plasma and projectile is not completely elastic since the projectile is ablated to some degree. The inelastic collision will result in a slower velocity projectile, however, so that the elastic collision calculation is the most favorable from the point of view of determining maximum possible particle velocity.

It has been determined that the coaxial plasma accelerator is not a suitable device to propel projectiles to velocities of the order of

20 kilometers/second unless the accelerator is modified in a way which will increase the plasma density.

Several techniques have been tried for increasing the plasma density (e.g., converging nozzles of dielectric and conducting materials).

When a stainless steel nozzle was used, no beads striking the target were detected. It was noted that spherules of condensed aluminum, 1 to 2 millimeters in diameter, appeared on the wall of the nozzle after the gun was fired. Since it appeared that too much energy was absorbed from the plasma by the stainless steel nozzle walls, a dielectric material was tried.

A nozzle was constructed with a commercially available material called "Grade-A Lava." When this nozzle was used, velocities of 2.3 kilometers/second were attained with 1.05×10^{-2}-centimeters diameter glass beads. Although the walls of the nozzle were blackened, no noticeable deposit of aluminum on the nozzle wall was detected. However, since the velocity attainable was only about 10 percent of the desired velocity, it was necessary to find a different way to increase the plasma density.

A coil wound in a conical shape, concentric about the longitudinal axis of the gun and energized by the plasma itself, has accelerated glass beads of 0.66-millimeter diameter to velocities of 7 to 8 kilometers/second and beads of smaller diameter to still higher velocities. The theory of the coil has not yet been fully developed but is under investigation.

CHAPTER VI

SUMMARY AND CONCLUSIONS

Summary

It has been shown that the simple circuit theory of the coaxial plasma generator is not sufficient to adequately explain the physical phenomena which occur when the plasma generator is loaded with a disc of conducting material and then energized. In particular it has been shown that the magnetic fields developed by the current flowing in the disc are not of sufficient strength to keep the disc from exploding.

It has also been shown that this coaxial plasma generator is not suitable for accelerating projectiles of a useful size range to velocities of the order of 20 kilometers/second unless some means of increasing the plasma density is used.

It has also been experimentally determined that when the density of the plasma is increased, projectiles of a useful size range and velocity have been produced.

Conclusions

By utilizing the coaxial plasma generator and a self-energized plasma-containment coil, a useful device may be designed for accelerating small projectiles to hypervelocities in the range of 20 kilometers/second.

The theoretical understanding of this system and the parameters to be varied to obtain predicted results have yet to be discovered.

APPENDIX A

INDUCTANCE AND CAPACITANCE OF COAXIAL CONDUCTORS

For a hollow conducting cylinder carrying a current the magnetic field at the points P and P' of Figure A-1 can be calculated from the Biot-Savart law, where

$$\overline{dB} = \frac{\mu_o I}{4\pi} \frac{\overline{d\ell} \times \overline{w}}{w^3} .$$

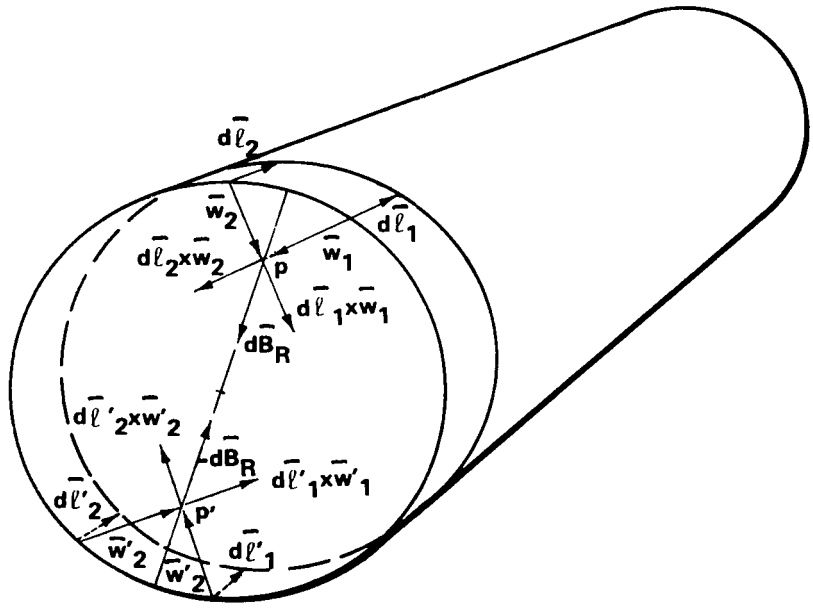

FIGURE A-1. HOLLOW CONDUCTING CYLINDER

Referring to Figure A-1, points P and P' lie on a diameter and are equally distant from the longitudinal axis of the cylinder. Consider pairs of current elements, $Id\ell_1$ and $Id\bar{\ell}_2$, and $Id\bar{\ell}'_1$ and $Id\bar{\ell}'_2$ where I is the current per unit length of perimeter of the cylinder, and use the Biot-Savart equation to compute the resulting fields

$$\bar{dB} = \frac{\mu_o I}{4\pi}\left(\frac{\bar{d\ell}_1 \times \bar{w}_1}{w_1^3} + \frac{\bar{d\ell}_2 \times \bar{w}_2}{w_2^3}\right)$$

and

$$\bar{dB}' = \frac{\mu_o I}{4\pi}\left(\frac{\bar{d\ell}'_1 \times \bar{w}'_1}{w_1'^3} + \frac{\bar{d\ell}'_2 \times \bar{w}_2'}{w_2'^3}\right) \quad .$$

Since the magnitudes of the $\bar{d\ell}$ and $\bar{w}$ terms are such that

$$d\ell_1 = d\ell_2 = d\ell_1' = d\ell_2' \quad \text{and} \quad w_1 = w_2 = w_1' = w_2' \quad ,$$

the only nonzero components of $\bar{dB}$ and $\bar{dB}'$ are dB_R and dB_R', and since these are components of oppositely directed vectors along the diameter, the vector sum is

$$\bar{dB} = \hat{r}\, dB_R - \hat{r}\, dB_R' = 0 \quad .$$

Therefore, if all current elements are calculated for every pair of interior points of the cylinder, the resultant magnetic field will be zero. There is no magnetic field within a hollow-conducting cylinder carrying a longitudinal current.

The field surrounding the center conductor of a coaxial line may be found using the circuital form of Ampere's law, where

$$\oint \bar{B} \cdot d\bar{\ell} = \mu_o I$$

for a path linking the current. For a path tangential to the field

$$\oint \bar{B} \cdot d\bar{\ell} = B \oint d\ell$$

and

$$B \oint d\ell = 2\pi rB$$

for a circular path.

Then,

$$\mu_o I = 2\pi B r \quad ,$$

or

$$B = \frac{\mu_o I}{2\pi r} \quad .$$

These results may now be used to find the inductance of a coaxial pair of conductors. The total magnetic flux linkage for a length Z is

$$\Lambda = z \int_a^b B\, dr = z \frac{\mu_o I}{2\pi} \int_a^b \frac{dr}{r}$$

$$\Lambda = \frac{z \mu_o I}{2\pi} \ln \frac{b}{a} \quad .$$

The inductance L is defined as

$$L \equiv \frac{\Lambda}{I} = \frac{\mu_o z}{2\pi} \ln \frac{b}{a} \quad ,$$

and the inductance per unit length is

$$\lambda = \frac{L}{z} = \frac{\mu_o}{2\pi} \ln \frac{b}{a} \quad .$$

To calculate the capacitance for the coaxial conductors, start with Maxwell's equation, where

$$\overline{\nabla} \cdot \overline{D} = \rho$$

$$\overline{\overline{\nabla}} \cdot \overline{E} = \frac{\rho}{\epsilon_o} \quad .$$

From the integral form of Gauss'law,

$$\int \overline{E} \cdot d\bar{s} = \int \frac{\rho}{\epsilon_o} \, d\tau = \frac{Q_L}{\epsilon_o} \quad ,$$

where the charge Q_L is a line charge density, or

$$E_r(2\pi r) = \frac{Q_L}{\epsilon_o} \quad ,$$

since

$$\int ds = 2\pi r$$

per unit length. Then,

$$E_r = \frac{Q_L}{2\pi \epsilon_o r} \quad .$$

Since

$$\overline{E} = -\overline{\nabla} V$$

and

$$E_r = -\frac{dV}{dr} \quad ,$$

or

$$-\int_{V_{r_o}}^{V_{R_{max}}} dV = \int_{r_o}^{R_{max}} E_r \, dr \quad ,$$

and, if

$$V_{R_{max}} = 0 \quad ,$$

then

$$V_{r_o} = \int_{r_o}^{R_{max}} \frac{Q_L}{2\pi\epsilon_o} \frac{dr}{r} = \frac{Q_L}{2\pi\epsilon_o} \ln \frac{R_{max}}{r_o} \quad .$$

By definition,

$$C \equiv \frac{Q}{V} \quad ,$$

so that the capacitance of the coaxial cable is

$$C = \frac{2\pi\epsilon_o}{\ln \frac{R_{max}}{r_o}} \quad \text{farad/meter} \quad .$$

APPENDIX B

LCR CIRCUIT THEORY

For the circuit consisting of an inductance L, a capacitance C, and a resistance R connected in series, the differential equation describing the circuit is

$$L \frac{di}{dt} + i R + \frac{q}{C} = 0 \quad .$$

Now $i = \frac{dq}{dt}$, so that

$$L \frac{d^2q}{dt^2} + R \frac{dq}{dt} + \frac{q}{C} = 0 \quad ,$$

and, by differentiation,

$$L \frac{d^2i}{dt^2} + R \frac{di}{dt} + \frac{i}{C} = 0 \quad ,$$

then

$$L \frac{d^2q}{dt^2} + R \frac{dq}{dt} + \frac{q}{C} = 0$$

has a solution of the form $Q = A(\exp \gamma t)$. Then, substituting into the differential equation,

$$L \gamma^2 + R\gamma + \frac{1}{C} = 0 \quad ,$$

so that

$$\gamma = -\frac{R}{2L} \pm \sqrt{\frac{R^2}{4L^2} - \frac{1}{LC}} \quad .$$

Letting

$$\alpha \equiv \frac{R}{2L}$$

and

$$\beta \equiv \pm\sqrt{\frac{R^2}{4L^2} - \frac{1}{LC}} \quad ,$$

then

$$\gamma = -\alpha \pm \beta \ ,$$

so

$$q = (\exp - \alpha t)\,[A_1(\exp \beta t) + A_2(\exp - \beta t)]$$

and

$$i = (\exp - \alpha t)\,[(\beta - \alpha)\,A_1\,(\exp \beta t) - (\beta + \alpha)\,A_2(\exp - \beta t)] \quad .$$

Now $q = q_o$ and $i = 0$ at $t = 0$, or $q_o = A_1 + A_2$, and

$$(\beta - \alpha)A_1 = (\beta + \alpha)A_2 \ ,$$

$$A_2 = -\frac{\alpha - \beta}{2\beta}\, q_o \ ,$$

and

$$A_1 = \frac{\alpha + \beta}{2\beta}\, q_o \quad .$$

Then,

$$q = \frac{q_o}{2\beta} (\exp - \alpha t) [(\alpha+\beta)(\exp \beta t) - (\alpha-\beta)(\exp -\beta t)] \quad .$$

If β is complex, then

$$\frac{R^2}{4L^2} - \frac{1}{LC} < 0 \quad ,$$

or

$$R^2 < 4 \frac{L}{C} \quad ,$$

and a periodic solution is possible.

If a solution is assumed for q• where

$$q = A_o (\exp - \alpha t) \sin (\omega_o t + \varphi) \quad ,$$

and is substituted into the differential equation

$$\left[(\alpha^2-\omega_o^2) L - \alpha R + \frac{1}{C}\right] \sin(\omega_o t + \varphi) + (-2\alpha\omega_o L + \omega_o R)\cos(\omega_o t+\varphi) = 0 \quad .$$

Then

$$\omega_o = \sqrt{\frac{1}{LC} - \frac{R^2}{4L^2}}$$

Using the initial conditions

$$q_o = A_o \sin \varphi$$

and

$$\omega_o \cos \varphi - \alpha \sin \varphi = 0 \quad ,$$

then

$$\tan \varphi = \frac{\omega_o}{\alpha} \quad , \quad A_o = \frac{q_o}{\sin \varphi} = \frac{\sqrt{\omega_o^2 + \alpha^2}}{\omega_o} \quad q_o \quad ,$$

or

$$i = \frac{\sqrt{\omega_o^2 + \alpha^2}}{\omega_o} q_o (\exp - \alpha t)[\omega_o \cos(\omega_o t + \varphi) - \alpha \sin(\omega_o t + \varphi)]$$

By expanding,

$$i = -\left(\frac{\omega_o^2 + \alpha^2}{\omega_o}\right) q_o (\exp - \alpha t) \sin \omega_o t \quad ,$$

or

$$i = i_o (\exp - \alpha t) \sin \omega_o t \quad ,$$

where

$$i_o = -\left(\frac{\omega_o^2 + \alpha^2}{\omega_o}\right) q_o$$

and

$$\nu_o = \frac{\omega_o}{2\pi} = \frac{1}{2\pi} \sqrt{\frac{1}{LC} - \frac{R^2}{4L^2}} \quad .$$

To find the time when the current has an extremum value, differentiate the expression

$$i = -\left(\frac{\omega_o^2 + \alpha^2}{\omega_o}\right) q_o (\exp - \alpha t) \sin \omega_o t$$

is differentiated and the derivative set equal to zero. Then,

$$\tan \omega_o t_{max} = \frac{\omega_o}{\alpha} \quad .$$

Since there are recurring maxima and minima, the time interval between successive maxima is

$$\omega_o (t_{max} + T_o) = \omega_o t_{max} + 2\pi \quad ,$$

where

$$T_o = \frac{2\pi}{\omega_o} = \frac{2\pi}{\sqrt{\frac{1}{LC} - \frac{R^2}{4L^2}}} \quad .$$

If i' and i'' are two successive maxima of current, then

$$\frac{i'}{i''} = \frac{(\exp - \alpha t)}{(\exp[-\alpha t - \alpha T_o]} = \exp \alpha T_o$$

and

$$\ln \frac{i'}{i''} = \alpha T_o = \frac{2\pi \left(\frac{R}{2L}\right)}{\sqrt{\frac{1}{LC} - \frac{R^2}{4L^2}}} \quad .$$

APPENDIX C

COMPUTER PROGRAM

A fourth-order Runge-Kutta integration scheme written in MARVES language [12] was used to solve the coupled circuit equations

$$(L_o + \lambda x)\ \frac{d^2V}{dt^2} + \left(R_o + R_1 x + R_2 + \lambda\ \frac{dx}{dt}\right) \frac{dV}{dt} + \frac{V}{C} = 0$$

and

$$\frac{d^2x}{dt^2} = \frac{L_o + \lambda x_o}{V_o{}^2 \lambda}\ \left(\frac{dV}{dt}\right)^2 \quad .$$

The variable and constant names used in the program are:

L_o = L0

λ = LAMBDA

x = X

$\frac{d^2V}{dt^2}$ = DDVT

R_o = R0

R_1 = R1

R_2 = R2

$\frac{dx}{dt}$ = DXT

$\frac{d^2x}{dt^2}$ = DDXT

$\frac{dV}{dt}$ = DVT

V = V

C = C

t = TIME

The computed current was

CUR = - (C) (DVT).

The flow chart for the main program is shown in Figure C-1. The subroutine SETONE flow chart is shown in Figure C-2. Within the SETONE subroutine is a Simpson's rule integration of the quantity I^2R_2 which provides a calculated energy dissipation for the plasma. The integration is carried out over a time period equal to the duration of the first half-cycle of the current discharge curve (Fig. 9).

The Simpson's rule integration is called SIMPSO and is called out in subroutine SETONE as SIMPSO. The SIMPSO subprogram flow chart is shown in Figure C-3. The flow chart for subroutine SETTWO is shown in Figure C-4. The computer program listing is also included.

MAIN PROGRAM
COMMENT: LANGUAGE FORTRAN

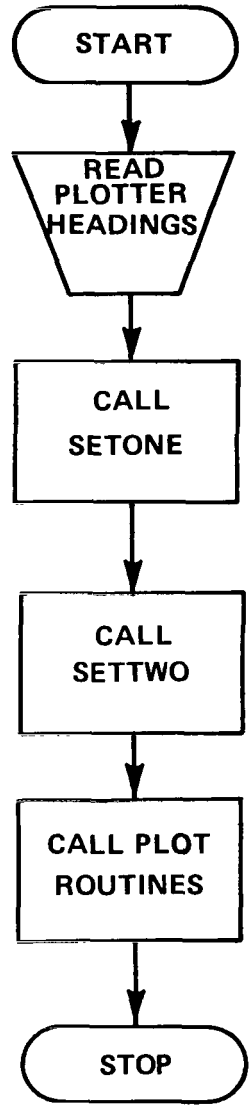

FIGURE C-1. COMPUTER MAIN PROGRAM

SUBROUTINE SETONE

COMMENT: DIFFERENTIAL EQUATIONS FOR X ≤0.67 AND
TIME ≤200 μ
LANGUAGE MARVES

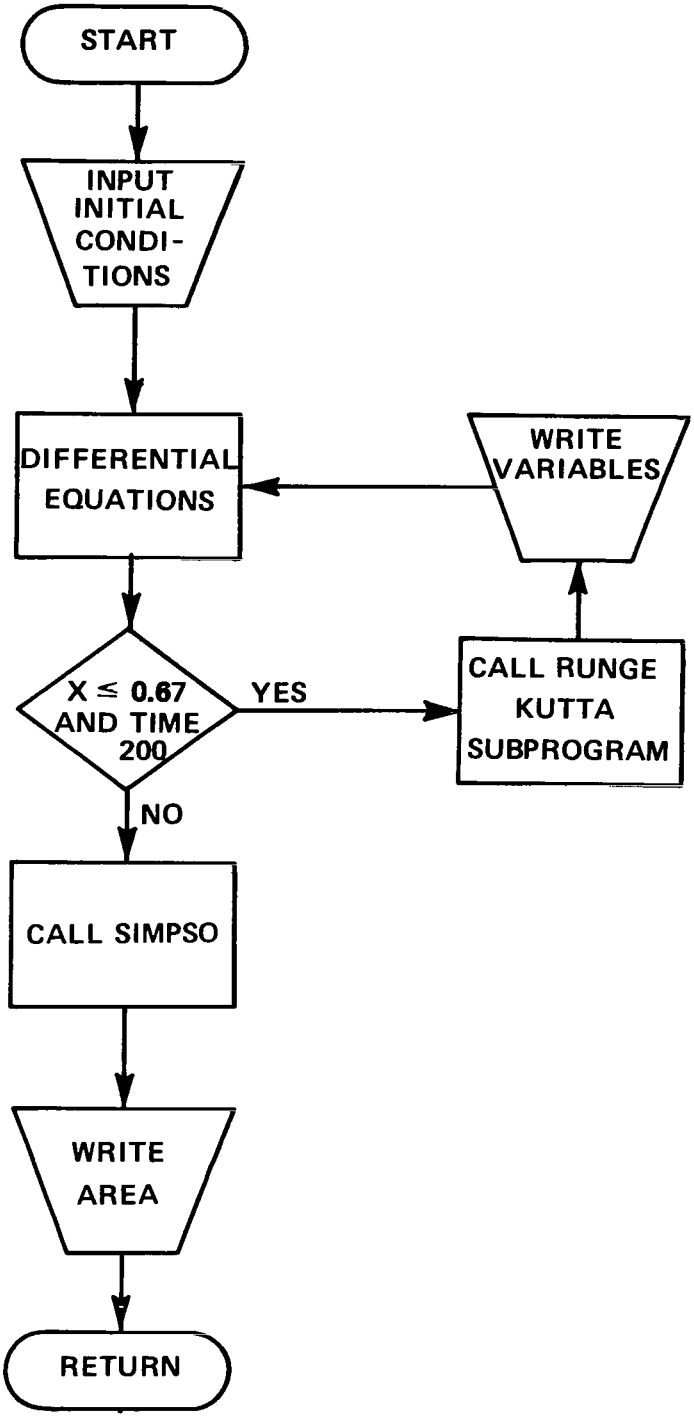

FIGURE C-2. COMPUTER SETONE PROGRAM

COMMENT: SIMPSON'S RULE
LANGUAGE FORTRAN

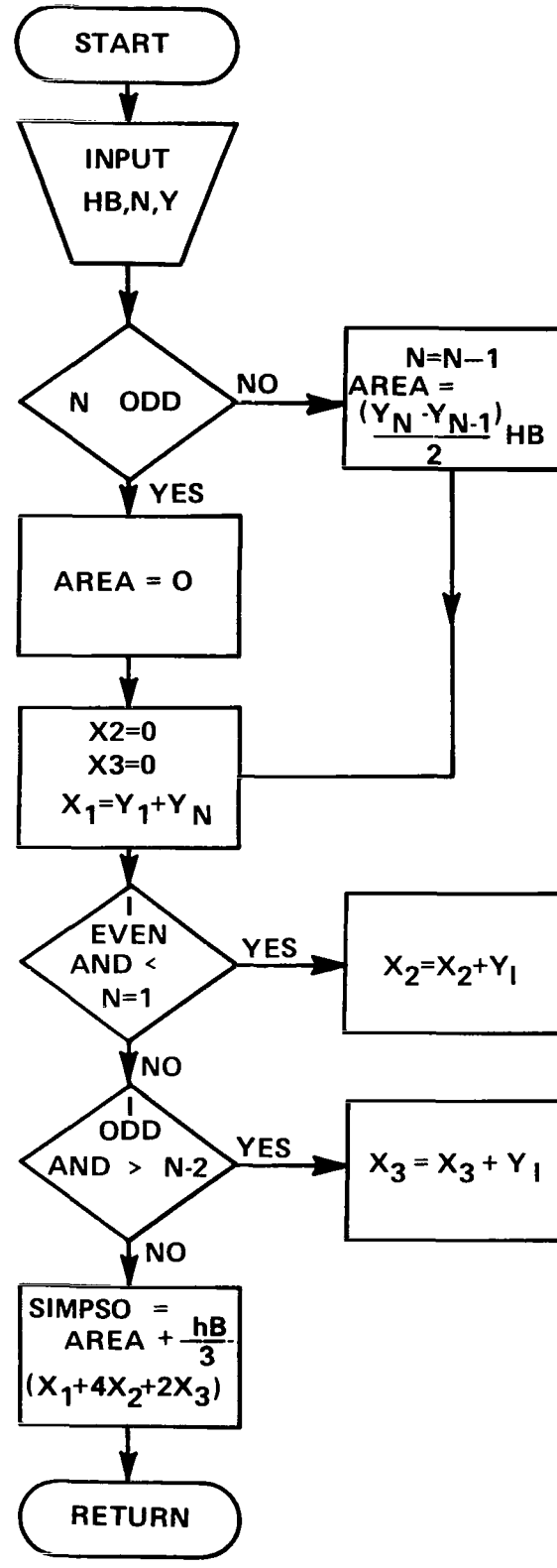

FIGURE C-3. COMPUTER SIMPSO PROGRAM

SUBROUTINE SETTWO
COMMENT: DIFFERENTIAL EQUATIONS FOR X > 0.67 AND TIME ≤ 200 μ sec
LANGUAGE MARVES I

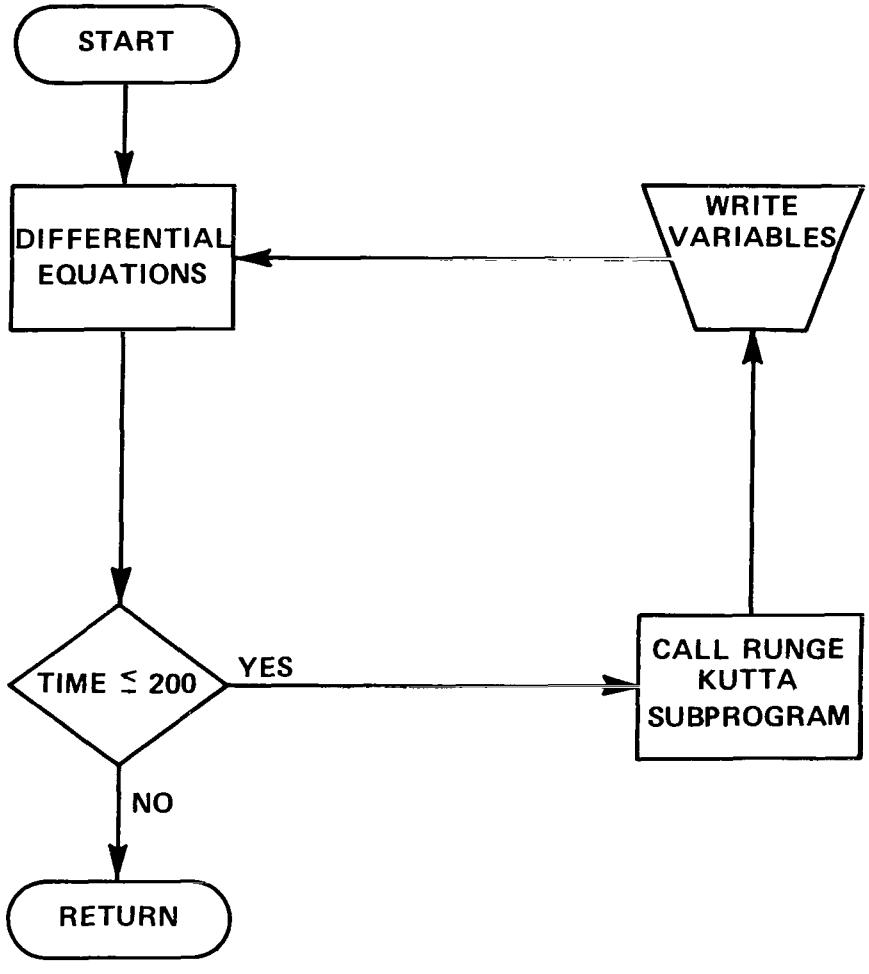

FIGURE C-4. COMPUTER SETTWO PROGRAM

```
00101     1*          REAL LO,LAMBDA
00103     2*          COMMON/BLOCK1/LO,LAMBDA,RO,R1,R2,C,CONST/BLOCK2/V,DVT,DDVT,X,DXT,
00103     3*         $DDXT,TIME,DTSTEP
00104     4*          DIMENSION CUR1(400),TIME1(400),FLDX(12),FLDY(12),FLDZ(12)
00105     5*          COMMON/BLOCK3/CUR1,TIME1,NUMBER
00106     6*          CALL IDENT(1)
00107     7*          READ(5,1)FLDX,FLDY,FLDZ
00125     8*        1 FORMAT(12A6/12A6/12A6)
00126     9*          CALL SETONE
00127    10*          CALL SETTWO
00130    11*          DO 10 I = 1,NUMBER
00133    12*       10 CUR1(I) = -CUR1(I)
00135    13*          CALL QUIK3L(-1.0,200.,-3.,3.,1H*,FLDX,FLDY,-NUMBER,TIME1,CUR1)
00136    14*          DO 2 I = 1,NUMBER
00141    15*        2 CUR1(I) = CUR1(I)*1.E+5

00143    16*          CALL QUIK3L(-1.0,200.,-3.E5,3.E5,1H*,FLDX,FLDZ,-NUMBER,TIME1,CUR
00143    17*         $1)
00144    18*          CALL ENDJOB
00145    19*          STOP
00146    20*          END

      END OF COMPILATION:        NO   DIAGNOSTICS.
```

```
      SUBROUTINE SETONE
      REAL LO,LAMBDA
      COMMON/BLOCK1/LO,LAMBDA,RO,R1,R2,C,CONST/BLOCK2/V,DVT,DDVT,X,DXT,
     $DDXT,TIME,DTSTEP
      DIMENSION CUR1(400),FCUR(200),TIME1(400)
      COMMON/BLOCK3/CUR1,TIME1,NUMBER
      INITIALIZE
      NUMBER = 0
      INTEGRATION ACCURACY = .6
      SKIP PAGE
    3 CONTINUE
      INPUT NAMELIST(5,NAME1)LO,LAMBDA,RO,R1,R2,C,V,X,DVT,DXT,TIME,DTSTE
     $P
      DTSTEP = DTSTEP/10.
    6 CONTINUE
      OUTPUT TITLE RUNGE KUTTA INTEGRATION
      SKIP LINE
      CONST = (LO + LAMBDA*X)/(V**2*LAMBDA)
      OUTPUT TITLE DEFINED AND CALCULATED CONSTANTS
      SKIP LINE
      OUTPUT LIST LO,LAMBDA,RO,R1,R2/C,CONST
      SKIP LINE
      OUTPUT TITLE INITIAL CONDITIONS
      SKIP LINE
      OUTPUT LIST TIME,DXT,X,DVT,V
      SKIP LINE
      DIFFERENTIAL EQUATIONS
    2 DDXT = CONST*DVT**2
      DDVT = -((R2 + RO + R1*X + LAMBDA*DXT)*DVT + V/C)/(LO + LAMBDA*X)
    1 CONTINUE
      INTEGRATION
      METHOD RUNGE KUTTA   ORDER = 2,X,DXT,DDXT,V,DVT,DDVT
      EVENTS
      C1 = DXT
      CUR = -C*DVT
      OUTPUT LIST TIME,V,CUR,DXT,X
      NUMBER = NUMBER + 1
      FCUR(NUMBER) = CUR**2*R2
      CUR1(NUMBER) = CUR/1.E+5
      TIME1(NUMBER) = TIME*1.E+6
      IF(X.GE.0.67)GO TO 7
      EVENT(EXIT)TIME = 2.E-3
      TERMINAL COMPUTATIONS
    7 AREA = SIMPSO(DTSTEP,NUMBER,FCUR)
      SKIP PAGE
      OUTPUT LIST AREA
      RETURN
      END
```

```
00101      1*          FUNCTION SIMPSO(HB,N,Y)
00103      2*          DIMENSION Y(N)
00104      3*          N2 = N/2
00105      4*          N3 = (N + 1)/2
00106      5*          IF(N2.NE.N3)GO TO 19
00110      6*          AREA = (Y(N) - Y(N - 1))*HB/2.
00111      7*          N = N - 1
00112      8*          GO TO 20
00113      9*       19 AREA = 0.
00114     10*       20 X1 = Y(1) + Y(N)
00115     11*          X2 = 0.
00116     12*          X3 = 0.
00117     13*          N1 = N - 1
00120     14*          DO 1 I = 2,N1,2
00123     15*        1 X2 = X2 + Y(I)
00125     16*          N2 = N1 - 1
00126     17*          DO 2 I = 3,N2,2
00131     18*        2 X3 = X3 + Y(I)
00133     19*          SIMPSO = (HB/3.)*(X1 + 4.*X2 + 2.*X3)+ AREA
00134     20*          RETURN
00135     21*          END

       END OF COMPILATION:         NO  DIAGNOSTICS.
```

```
1*          SUBROUTINE SETTWO
2*          REAL LO,LAMBDA
3*          COMMON/BLOCK1/LO,LAMBDA,RO,R1,R2,C,CONST/BLOCK2/V,DVT,DDVT,X,DXT,
4*         $DDXT,TIME,DTSTEP
5*          DIMENSION CUR1(400),TIME1(400)
6*          COMMON/BLOCK3/CUR1,TIME1,NUMBER
7*          INITIALIZE
8*          DTSTEP = DTSTEP*10.
9*          INTEGRATION ACCURACY = 16
10*         SKIP PAGE
11*         OUTPUT LIST LO,LAMBDA,RO,R1,R2/C,CONST
12*         SKIP LINE
13*         OUTPUT LIST TIME,DVT,V,DXT,X
14*         SKIP LINE
15*         DIFFERENTIAL EQUATIONS
16*         DDVT = -((RO + R2 + R1*0.67)*DVT + V/C)/(LO + 0.67*LAMBDA)
17*         INTEGRATION
18*         METHOD RUNGE KUTTA ORDER = 2,V,DVT,DDVT
19*         EVENTS
20*         CUR = -C*DVT
21*         OUTPUT LIST TIME,V,CUR
22*         NUMBER = NUMBER + 1
23*         TIME1(NUMBER) = TIME*1.E+6
24*         CUR1(NUMBER)= CUR/1.E+5
25*         EVENT(EXIT)TIME = 2.E-4
26*         TERMINAL COMPUTATIONS
27*         RETURN
28*         END
```

APPENDIX D

BEHAVIOR OF AN IONIZED DISC CONDUCTOR IN A COAXIAL PLASMA ACCELERATOR

The magnetic fields within the ionized disc have been calculated and shown to be clockwise when viewed facing the disc. The fields are directed oppositely on the two sides of the disc.

The magnetic pressure term arising from these magnetic fields has been calculated for the particular conditions described in the body of this report. The pressure has been shown to be 36 times as high near the center electrode as it is near the outer electrode. The pressure is caused by the magnetic fields within the disc which create a force inward on the current on both sides of the disc.

The magnetic field created by the current flowing in the center electrode of the coaxial accelerator toward the disc creates a magnetic field around the center electrode in the same direction as the field on the inner disc face caused by the current in the disc. The field of the center electrode has a magnitude of (Appendix A)

$$B = \frac{\mu_o I}{2\pi r} \quad .$$

The charged particles are acted upon by the $\bar{j} \times \bar{B}$ forces arising from the current in the disc and the magnetic field created by the current in the center electrode. Thus, the magnetic pressures created by the superposed fields force the charged particles of the disc to travel toward the muzzle of the coaxial accelerator.

It is assumed that some of the energy acquired from the capacitors by the charged particles is exchanged with the neutral particles causing the neutral particles to diffuse into the accelerator. Also, as the charged particles are being driven to the muzzle of the accelerator the neutral particles diffuse into the region which has been vacated.

The diffusion of the neutral particles can be described by the following equation:

$$J_{q_\ell} = - D \frac{dn_o}{dq_\ell}$$

where J_{q_ℓ} is the flux of particles in the q_ℓ direction, D is the diffusion coefficient, and $\frac{dn_o}{dq_\ell}$ is the density gradient of particles. The neutral gas can diffuse in all directions but will diffuse most rapidly in the direction of highest density gradient. Since the highest density gradient occurs in the negative z direction the neutral gas will expand most rapidly in a direction away from the muzzle.

The neutral gas is relatively hot and will produce some ionization by collision processes between neutral particles. If the density is sufficiently

high to sustain an arc the electrical discharge will spread throughout the volume of the coaxial accelerator. The discharge will continue until the gas density becomes too low to sustain the arc, or until the energy stored in the capacitor bank has been dissipated.

REFERENCES

1. Christman, D. R.; Gehring, J. W.; Maiden, C. J.; and Wenzel, A. B. Study of the Phenomena of Hypervelocity Impact. Summary Report for NASA Contract NAS8-5067, George C. Marshall Space Flight Center, Huntsville, Alabama 1963, (Prepared by General Motors Defense Research Laboratories, Santa Barbara, California, Report Number TR63-216).

2. Mostov, P. M.; Neuringer, J. H.; and Rigney, D. S. "Electromagnetic Acceleration of a Plasma Slug," Phys. Fluids, vol. 4, no. 9 (1961), pp. 1097 - 1104.

3. Artsimovich, L. A.; Luk'Ianov, S. IV.; Podgoinyi, I. M.; and Chuvalin, S. A. "Electrodynamic Acceleration of Plasma Bunches." Sov. Phys-JETP, vol. 6, no. 1 (1958), pp. 1-51.

4. Igenbergs, E. B. Voruntersuchungen uber die Beschlenigung von stark erhitzen Ionisierten Gasen durch ein elektromagnetisches Feld. Bericht, Nr. 64/1, Institut fur Stromung Smechanik Technische Hochschule, Munchen (1964).

5. Lovberg, R. H.; Hayworth, B.; and Gooding, T. The Use of a Coaxial Gun for Plasma Propulsion. Report Number AE62-0678, NASA-Lewis Research Center, 1962.

6. Touloukian, Y. S. Thermophysical Properties of High Temperature Solid Materials. New York: MacMillian Co., 1967.

7. Stratton, J. A. Electrodynamic Theory. New York: McGraw-Hill, 1941.

8. Jackson, J. D. Electrodynamics. New York: John Wiley & Sons, 1962.

9. Bruce, R. E. A Model and Calculation for the Properties of an Exploding Plasma Sphere. Doctoral Thesis, Oklahoma State University, Stillwater, Oklahoma, 1966.

10. Peery, L. J. A Model and Calculation for Laser Induced Plasmas. Doctoral Thesis, Oklahoma State University, Stillwater, Oklahoma, 1970.

11. Willis, H. W. Analytical and Experimental Investigations of the Transient Properties of Dense Aluminum Plasmas. Doctoral Thesis, Oklahoma State University, Stillwater, Oklahoma, 1971.

12. Davidson, M. C., and Setter, R. M. MARVES Marshall Vehicle Engineering Simulation. Users manual, NASA, George C. Marshall Space Flight Center, Oct. 15, 1969.

BIBLIOGRAPHY

Johnson, R. G.; Caldwell, W. C.; Hudson, D. E.; and Spedding, F. H. "A Mass Spectrometric Positive Ion Technique for Determining Phase Transition Temperatures and Heats of Transformation in Metals." Phys. Rev., vol. 91, no. 466A (1953).

Krause, J. D. Electromagnetics. New York: McGraw-Hill, 1953.

Lyman, T. Metals Handbook. Vol. I, Eighth Ed., American Society for Metals, 1961.

J. M., Meek, and Craggs, J. D. Electrical Breakdown of Gases. London: Oxford at the Clarendon Press, 1953.

Page, L. and Adams, N. I. Principles of Electricity. New York: D. Van Nostrand Co., 1950.

NASA-Langley, 1972 —— 25

"The aeronautical and space activities of the United States shall be conducted so as to contribute . . . to the expansion of human knowledge of phenomena in the atmosphere and space. The Administration shall provide for the widest practicable and appropriate dissemination of information concerning its activities and the results thereof."

—NATIONAL AERONAUTICS AND SPACE ACT OF 1958

NASA SCIENTIFIC AND TECHNICAL PUBLICATIONS

TECHNICAL REPORTS: Scientific and technical information considered important, complete, and a lasting contribution to existing knowledge.

TECHNICAL NOTES: Information less broad in scope but nevertheless of importance as a contribution to existing knowledge.

TECHNICAL MEMORANDUMS: Information receiving limited distribution because of preliminary data, security classification, or other reasons.

CONTRACTOR REPORTS: Scientific and technical information generated under a NASA contract or grant and considered an important contribution to existing knowledge.

TECHNICAL TRANSLATIONS: Information published in a foreign language considered to merit NASA distribution in English.

SPECIAL PUBLICATIONS: Information derived from or of value to NASA activities. Publications include conference proceedings, monographs, data compilations, handbooks, sourcebooks, and special bibliographies.

TECHNOLOGY UTILIZATION PUBLICATIONS: Information on technology used by NASA that may be of particular interest in commercial and other non-aerospace applications. Publications include Tech Briefs, Technology Utilization Reports and Technology Surveys.

Details on the availability of these publications may be obtained from:

SCIENTIFIC AND TECHNICAL INFORMATION OFFICE

NATIONAL AERONAUTICS AND SPACE ADMINISTRATION

Washington, D.C. 20546